©2001 Uspekhi Fizicheskikh Nauk, Russian Academy of Sciences

REVIEWS OF TOPICAL PROBLEMS

PACS numbers: 61.72.Lk, **62.25.+g**, 73.40.Kp, **81.15.+z**

Silicon – germanium epilayers: physical fundamentals of growing strained and fully relaxed heterostructures

Yu B Bolkhovityanov, O P Pchelyakov, S I Chikichev

DOI: 10.1070/PU2001v044n07ABEH000879

Contents

1. **Introduction** 655
2. **Plastic relaxation** 655
   2.1 Threading and misfit dislocations; 2.2 Critical thickness for the injection of misfit dislocations; 2.3 Propagation of threading dislocations in strained epilayers. Theory and experiment; 2.4 Propagation of misfit dislocations in strained epilayers. Theory and experiment; 2.5 Plastic relaxation of epilayers; 2.6 Interaction of dislocations and multiplication. Secondary sources of misfit dislocations; 2.7 Buried epilayers and multilayer heterostructures. Special features of plastic relaxation
3. **Elastic relaxation** 668
   3.1 'Compliant' and 'soft' substrates; 3.2 Elastic relaxation of epilayers via island formation
4. **Surface morphology of relaxed epilayers** 674
5. **Practical realization of the relaxation mechanisms** 675
   5.1 The main physical prerequisites for using GeSi/Si heterostructures in devices; 5.2 Artificial substrates; 5.3 Silicon – germanium nanostructures with quantum dots
6. **Conclusion** 678
   References 679

Abstract. **Ge_xSi_{1-x}/Si heterostructures involving two elemental semiconductors are becoming an important element in microelectronics. Their epitaxial growth requires a detailed knowledge of the mechanisms of elastic and plastic deformations in continuous and island films both at the early stages of epitaxy and during the subsequent heat treatment. The present work is a systematic review of current ideas on the fundamental physical mechanisms governing the formation of elastically strained and plastically relaxed Ge_xSi_{1-x}/Si heterocompositions. In particular, the use of compliant and soft substrates and the epitaxial synthesis of nanometer-sized islands ('quantum dots') are discussed.**

1. Introduction

Growing heterostructures with a relatively large difference in the lattice parameters between the film and substrate and a low density of threading dislocations (TDs) by molecular beam epitaxy (MBE) is one of the most important goals of semiconductor materials science. Studies in this area of research have been going on for about two decades. The main problems concerning applications form three groups:

Yu B Bolkhovityanov, O P Pchelyakov, S I Chikichev
Institute of Semiconductor Physics, Siberian Division of the Russian Academy of Sciences
pros. Lavrent'eva 13, 630090 Novosibirsk, Russian Federation
Tel./Fax (7-3832) 33-35 02
E-mail: pch@isp.nsc.ru

Received 17 October 2000
Uspekhi Fizicheskikh Nauk **171** (7) 689 – 715 (2001)
Translated by E Yankovsky; edited by S N Gorin

(1) Growing pseudomorphic epilayers and multilayer heterostructures without misfit dislocations (MDs). The stresses in such heterostructures modify the band structure of the semiconductor, which leads to new electrical and optical properties.

(2) The opposite problem, i.e., the growing of totally relaxed layers, known as artificial substrates, which is necessary in building various heterostructure devices based on materials whose lattice parameters differ from those of commercially available substrates. Here, the main goal is to achieve maximum structural perfection of such an artificial composite material, approaching in quality standard single-crystal substrates.

(3) An extreme manifestation of the relaxation of strained layers is the formation of nanometer-scale islands, a problem that has lately gained great popularity (purely scientific and also from the viewpoint of applications) in connection with the possibility of growing nanoisland ensembles with a density higher than 10^{10} cm^{-2} (ensembles of quantum dots). The special features of heteroepitaxial growth that lead to the realization of each of the three problems are based on general physical laws governing the relaxation of strained layers. The advances in understanding these laws in recent years are covered in the sections that follow.

2. Plastic relaxation

2.1 Threading and misfit dislocations

The substrate and layer are mismatched when their crystal unit cells differ in size. Since the formation of misfit dislocations requires additional energy, initially the layer grows in a strained, pseudomorphic state, in which the

dimensions of the layer and substrate cells in the interface plane are the same. After plastic relaxation is complete, the layer cell returns to its initial state and an MD network forms at the interface. In the ideal case, this is an orthogonal network of dislocations lying only in the interface plane or near it. However, as we will see shortly, such an MD network can be formed only when dislocations glide along inclined planes intersecting the layer. These dislocation branches intersecting the layer remain in it, thus forming a high density of TDs. In all the GeSi/Si heterostructures observed so far the MDs lie in $\langle 110 \rangle$ directions. There are two basic types of MD, which differ in the angle between the dislocation line and the direction of the Burgers vector, the angle being 60° and 90°. Accordingly, dislocations of the first type are called 60° dislocations and those of the second, 90° dislocations. For the 60° dislocations, the dislocation line and the Burgers vector lie in the $\{111\}$ plane, which for Ge and Si is the glide plane. This explains the preferred emergence of this type of dislocation in a relaxing stressed plane. The 90° dislocations (Lomer dislocations, or L dislocations) are sessile dislocations. From the viewpoint of energy, Lomer dislocations, being edge dislocations, are more suitable for layer relaxation than 60° dislocations, since for the former the fraction of the introduced plastic strain is twice as large as for the latter. However, since 90° dislocations cannot be introduced by gliding, the number of 90° MD is usually small.

In $Ge_xSi_{1-x}/Si(001)$ layers with small mismatches ($<1.5\%$), the MDs that form the orthogonal network are mostly of the 60° type. When the mismatches are large ($>2.3\%$), an orthogonal network of mostly short edge L dislocations is formed [1]. The nature of the dislocation microstructure at the interface of a plastically relaxed layer proves to greatly affect the perfection of the crystal structure of the bulk of the layer: short dislocations are linked to the layer's surface by TD branches, whose density reaches $10^{10}-10^{11}$ cm^{-2}. The problem of growing perfect, totally relaxed GeSi/Si layers breaks down into two problems: (a) to ensure the proper relaxation rate by injecting misfit dislocations, and (b) to reduce to a minimum the number of threading dislocations. To a certain extent these two problems contradict each other, since the injection of misfit dislocations occurs via the passage of threading dislocations through the bulk of the layer.

2.2 Critical thickness for the injection of misfit dislocations

In 1949, Frank and van der Merwe [2] suggested a way for growing a thin crystal layer on a substrate with a different lattice spacing without defects at the interface. In such a heteropair the mismatch between the layer and substrate spacings is compensated due to a change in the size of the layer cell, as a result of which the latter proves to be a biaxially strained pseudomorphic layer coherently interfaced with the substrate. The strain energy building up in the layer is proportional to the layer thickness. When the layer's thickness exceeds a certain value, known as the critical thickness, this energy becomes so high that a misfit dislocation appears at the interface, which partially or completely relieves the stresses in the bulk of the layer.

2.2.1 Energy-balance model. Let us discuss the energy-balance model based on the comparison of the energies of strained and plastically relaxed layers that was proposed by Matthews [3]. The stress energy of a unit area of a pseudomorphic layer of thickness h is given by the formula

$$E_\varepsilon = \frac{2G(1+\nu)}{1-\nu}\,\varepsilon^2 h\,, \qquad (1)$$

where G and ν are, respectively, the shear modulus and the Poisson ratio for an isotropic solid, and ε is the two-dimensional (plane) elastic strain in the layer due to the difference in the lattice parameters of the film and substrate

$$f = \frac{a_f - a_s}{a_s}\,. \qquad (2)$$

The energy of a unit area of the network of misfit dislocations plastically relaxing the layer is

$$E_d = \frac{2}{\rho}\,\frac{Gb^2(1-\nu\cos^2\alpha)}{4\pi(1-\nu)}\left(\ln\frac{\beta h}{b}+1\right). \qquad (3)$$

Here, the factor 2 stands for the two MD systems in each direction $\langle 110 \rangle$ along the interface, ρ is the number of dislocations per unit length in the interface plane, b is the length of the Burgers vector of a dislocation, and α is the angle between the Burgers vector and the dislocation line. The number β is called the dislocation core parameter, which, according to modern data, is taken equal to 0.76 (for 60° dislocations) [4]. The linear density of dislocations ρ plastically relaxing the layer is

$$\rho = \frac{b_{eff}}{f-\varepsilon}\,, \qquad (4)$$

where b_{eff} is the effective Burgers vector (i.e., the component of the Burgers vector in the interface plane in the direction perpendicular to a misfit dislocation, or the absolute plastic relaxation caused by the appearance of one misfit dislocation). Then

$$E_d = \frac{G(b/b_{eff})\,b(1-\nu\cos^2\alpha)}{2\pi(1-\nu)}\,(f-\varepsilon)\left(\ln\frac{\beta h}{b}+1\right). \qquad (5)$$

The total layer energy is $E_\varepsilon + E_d$. The value of the elastic strains of the layer ε^* at which this sum is at its minimum can be found from the expression $\mathrm{d}(E_\varepsilon + E_d)/\mathrm{d}\varepsilon = 0$ and is equal to

$$\varepsilon^* = \frac{(b/b_{eff})\,b(1-\nu\cos^2\alpha)}{8\pi h(1+\nu)}\left(\ln\frac{\beta h}{b}+1\right). \qquad (6)$$

The largest possible value of ε^* is f. Thus, the thickness of a pseudomorphic layer at which the first MD may appear, or the critical thickness, is

$$h_c = \frac{(b/b_{eff})\,b(1-\nu\cos^2\alpha)}{8\pi f(1+\nu)}\left(\ln\frac{\beta h_c}{b}+1\right). \qquad (7)$$

For a network of edge dislocations, $\alpha = 90°$ and $b/b_{eff} = 1$. For 60° dislocations, $\alpha = 60°$ and $b/b_{eff} = 2$. Allowing for the fact that, for the Ge_xSi_{1-x} system, $\nu = 0.28$, $f = 0.041x$ (where x is the concentration of Ge in the solid solution), and $\beta = 0.76$, in the case of 60° dislocations we arrive at the following simplified expression for the critical thickness:

$$h_c = 1.62\,\frac{b}{x}\left(\ln\frac{0.76h_c}{b}+1\right). \qquad (8)$$

2.2.2 Force-balance model. In 1974, Matthews and Blakeslee [5] proposed a model based on the balance of forces acting on a dislocation. Figure 1 schematically depicts the initial stage of the plastic relaxation of a pseudomorphic layer. The typical pattern is the generation in some manner of a 60° dislocation that can glide along a plane inclined with respect to the interface plane (111). The dislocation consists of a branch lying in the interface (a misfit dislocation) and a branch emerging from the layer's surface (a threading dislocation). The plastic relaxation of the layer is due to an increase in the length of each such misfit dislocation caused by the motion of the threading part in the glide plane. Each passage of this kind of dislocation loop through a portion of the layer lowers the elastic strain in this portion and, hence, under certain conditions, may prove to be energetically advantageous. Let us examine these conditions.

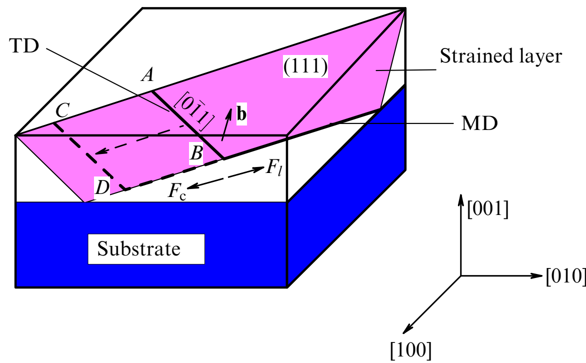

Figure 1. Schematic of plastic relaxation of a strained epilayer caused by formation of misfit dislocations and related threading dislocations.

On the threading part of the dislocation (the branch AB), there acts a force F_c facilitating the extension of the dislocation loop. This force is caused by misfit stresses that exist in the layer and can be written as follows [6]:

$$F_c = \frac{2G(1+\nu)}{1-\nu}\,\varepsilon b h \cos\lambda\,, \tag{9}$$

where λ is the angle between the Burgers vector and a line that lies in the interface plane and is perpendicular to the intersection of the dislocation glide plane and the substrate surface. Clearly, the force that facilitates dislocation propagation is proportional to the stresses in the layer and the layer thickness.

On the moving branch CD at point D, there acts a drag force F_l related to the additional work required for the formation of a new section (DB) of a misfit dislocation. The force is given by the formula

$$F_l = \frac{Gb^2(1-\nu\cos^2\alpha)}{4\pi(1-\nu)}\left(\ln\frac{\beta h}{b}+1\right). \tag{10}$$

The critical thickness is determined by the balance of these two forces: $F_c = F_l$. Hence,

$$h_c = \frac{b(1-\nu\cos^2\alpha)}{8\pi\varepsilon(1+\nu)\cos\lambda}\left(\ln\frac{\beta h_c}{b}+1\right). \tag{11}$$

Allowing for the fact that $\cos\lambda = 0.5$ [6] and that the greatest value of ε is f, we see that for the Ge_xSi_{1-x}-on-Si(001) system, this expression becomes identical to Eqn (8).

In more recent works devoted to the injection of misfit dislocations and the propagation of such dislocations in strained layers, the researchers have been using such concepts as the resolved shear stress τ and the effective, or excess, shear stress τ_{eff}. In Eqn (1), the factor τ_{eff} on the right-hand side is the 'plane' stress in the layer, σ. It is the rotation of this stress in the glide direction of the threading dislocation in the glide plane that is the resolved shear stress:

$$\tau = \cos\lambda\cos\phi\,\frac{2G(1+\nu)}{(1-\nu)}\,\varepsilon\,, \tag{12}$$

where ϕ is the angle between the glide plane and a normal to the interface. The product $\cos\lambda\cos\phi$ is known as the Schmid factor S. The shear component of the stress that inhibits the threading dislocation propagation is given by the formula [7]

$$\tau_s = \frac{Gb(1-\nu\cos^2\alpha)\cos\phi}{4\pi h(1-\nu)}\left(\ln\frac{\beta h}{b}+1\right). \tag{13}$$

The difference $\tau - \tau_s$ is called the effective shear stress τ_{eff} and is the driving force for TD propagation in strained layers of thickness h:

$$\tau_{\mathrm{eff}} = S\,\frac{2G(1+\nu)}{(1-\nu)}\,\varepsilon - \frac{Gb(1-\nu\cos^2\alpha)\cos\phi}{4\pi h(1-\nu)}\left(\ln\frac{\beta h}{b}+1\right). \tag{14}$$

From the fact that τ_{eff} is zero at the initial stage of plastic relaxation of layers, when $\varepsilon = f$, we can find the critical thickness:

$$h_c = \frac{b(1-\nu\cos^2\alpha)}{8\pi f(1+\nu)\cos\lambda}\left(\ln\frac{\beta h_c}{b}+1\right), \tag{15}$$

which coincides with Eqn (11).

2.2.3 Possibilities for controlling the predominant misfit dislocation type during heteroepitaxy. In 1980, Gutakovskiĭ et al. [8] derived a general equation for determining the pseudomorphic layer critical thickness for any law of change of elastic strain over the layer thickness. The researchers also constructed a polar diagram representing the dependence of the critical thickness on the orientation of the substrate surface. They found that partial misfit dislocations can be excluded from the process of heteroepitaxial stress relaxation by selecting an appropriate orientation of the substrate or by creating transition layers with a composition gradient. The calculations were carried out for the case of a continuous isotropic layer with a structure of the sphalerite (or diamond) type that coincided with that of the substrate and had the same elastic moduli, which remained constant from point to point. The researchers examined the most common mechanism of strain relaxation that realized itself through the dislocations slip.

Figure 2 depicts the results of the calculations done by Gutakovskiĭ et al. [8] by a polar diagram representing the dependence of the minimal critical thickness for the injection of misfit dislocations on the orientation of the substrate. The direction of the diagram's radius vector determines the direction of the normal to the substrate surface, while the length of this vector determines the minimum h_c for a given ε_0. Figure 2 combines two polar diagrams: the upper half, for the misorientation axis [011]; the lower half, for the axis [001].

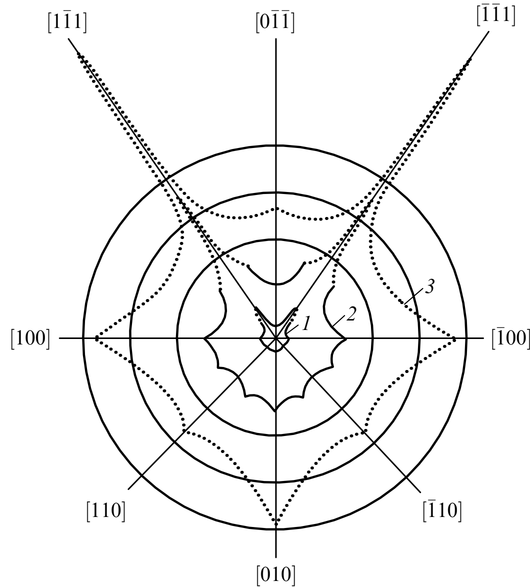

Figure 2. Polar diagram for the minimum critical thickness according to Gutakovskiĭ et al. [8]. The solid sections correspond to the formation of partial MDs and the dotted sections, to the formation of perfect MDs; ε_0 isequal to 4×10^{-2} (curve *1*), 1.5×10^{-2} (curve *2*), and 7×10^{-3} (curve *3*). The upper half of the diagram has been calculated for the misorientation axis [011], and the lower half, for [001]. The distance between the concentric rings for curves *1* and *2* amounts to 3 nm, and that for curve *3*, to 4.5 nm.

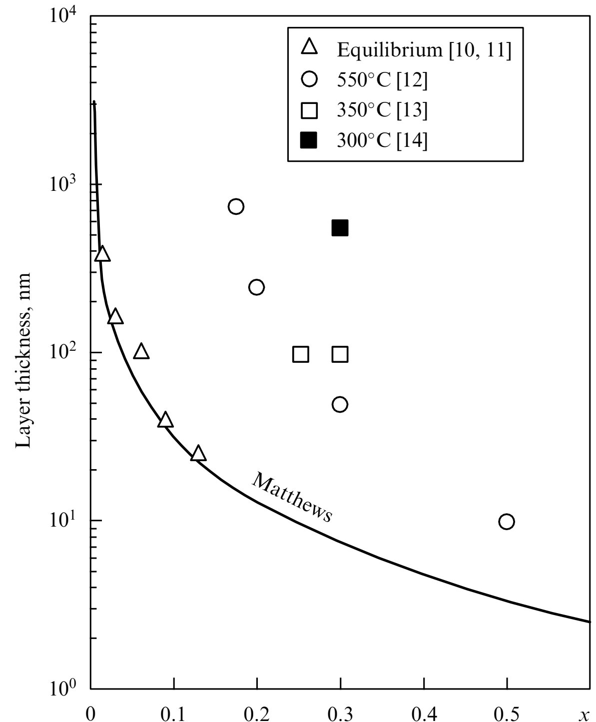

Figure 3. Critical thickness of $Ge_xSi_{1-x}/Si(001)$ layers as a function of the composition x. The solid curve represents the results obtained by formula (8), and the points represent the experimental data of various researchers for epilayers grown at different temperatures.

The polar diagram suggests that for sufficiently large values of $f = \varepsilon_0$ ($\sim 4 \times 10^{-2}$) the strain relaxation via perfect dislocations is preferable only within an extremely narrow range of substrate orientations (the deviation from (111) to (100) amounting to 2 – 7°). For all other orientations, partial MDs will be initially introduced. For small values of $f = \varepsilon_0$ ($\sim 7 \times 10^{-3}$), the formation of perfect MDs is energetically favorable at any orientation of the substrate. In the case of intermediate values of f ($\sim 1.5 \times 10^{-2}$), there are fairly broad ranges of orientations where either partial or perfect MDs are predominant, with the fraction of partial MDs increasing with decreasing stacking fault energy. The polar diagram also shows that the plastic strain is inhibited the most when the substrate is oriented exactly along {111} (h_c is at its maximum), especially at small values of ε_0. Hence, one can expect an elevated level of residual stresses, especially in thin layers.

2.2.4 The main experimental results. Figure 3 depicts a curve representing the theoretical dependence [Eqn (8)] of the critical thickness on composition for $Ge_xSi_{1-x}/Si(001)$ layers. In the second half of the 1980s and the beginning of the 1990s, there appeared a number of papers devoted to experimental measurements of the critical thickness for GeSi/Si layers and comparison of the data with the results of Matthews's calculations. Some experimental data on such measurements are also depicted in Fig. 3. For layers grown at high temperatures (900 °C) [9] or subsequently subjected to annealing [10, 11], the critical thickness determined through such experiments coincides fairly well with the theoretical curve (the small triangles in Fig. 3). The values of h_c determined in experiments with layers at lower temperature showed a stable excess over the calculated values, and the lower the temperature, the greater the excess [12 – 14]. An increase in h_c by a factor of ten or more was observed in these experiments, which is clearly visible in Fig. 3. After the fact that the critical thickness of the injection of misfit dislocations may substantially exceed the value given by Matthews's models had been thoroughly established, various interpretations of the phenomenon appeared. These interpretations were based on the assumption that the generation in, and the propagation of dislocations through, the layer are kinetically inhibited. The discussion of this problem will be continued in the sections that follow.

2.3 Propagation of threading dislocations in strained epilayers. Theory and experiment

The basic ideas of the theory of propagation of dislocations in crystals have been thoroughly studied in several monographs (e.g., see Ref. [15]). During the last fifteen years, several groups of researchers have studied dislocation propagation in GeSi/Si layers, e.g., Hull, Bean and coworkers [16 – 19] and Houghton and coworkers [20, 21], to name some. All these researchers based their investigations on studies involving bulk crystals of germanium and silicon [22 – 26]. The distinctive feature of the problem in question is the fact that the dislocations are in a biaxially compressed layer in which the stresses may be very high (> 1 GPa).

According to classical ideas [22], the expression for the dislocation propagation velocity can be written as follows:

$$V_d = V_0 \tau_{eff}^m \exp\left(-\frac{E_v}{kT}\right), \tag{16}$$

where V_0 is a constant, E_v is the activation energy of dislocation propagation via gliding, and τ_{eff} is the effective stress acting on the dislocation [Eqn (14)]. The effective stress

is proportional to ε (at the initial stage of relaxation, when $\varepsilon \sim f$, it is proportional to the difference in the lattice parameters of Ge and Si) and increases with the layer thickness h. Thus, the two parameters, ε and h, can be used to control the effective stress that determines the dislocation velocity at a given temperature.

Houghton [20] studied the propagation and nucleation of dislocations in strained layers of GeSi/Si(001) by the following method. Ge_xSi_{1-x} layers were grown at 350 – 500 °C to thicknesses exceeding h_c. Then, after a short period of isochronous annealing of the layers at higher temperatures, a dilute Schimmel etchant (four parts of 48% HF acid to five parts of 0.3 M solution of CrO_3) was applied to selectively etch (in the course of 30 – 60 s at 300 K [27, 28]) the surface of the annealed layers. This made it possible to establish traces of misfit dislocations, which were observed in a microscope fitted with a Nomarski attachment. The number of exposed traces was assumed equal to the originating misfit dislocations, and the length of these traces along the surface divided by the annealing time was assumed equal to twice the velocity of dispersal of the TD branches.

In the early studies of this problem, it was found that the dislocation velocities in bulk crystals of germanium and silicon change superlinearly with increasing effective stress and that the exponent m in equation (16) could vary from 1 to 1.5 [22]. Figure 4a (taken from Ref. [20]) demonstrates the TD gliding velocity as a function of the effective stress. On the basis of these data, the value of m was estimated as being 2 ± 0.1. By varying the annealing temperature, Houghton was able to estimate the TD dispersal velocity within a broad temperature range, which made it possible to determine the activation energy of dislocation propagation. Figure 4b depicts some curves representing the dependence of the dislocation velocity on the reciprocal temperature. The activation energy E_v, calculated from the slope of the curves in the ($\ln V - 1/T$) plane, was found to be independent of the germanium concentration (up to $x = 0.23$) and the effective stress τ_{eff} and was estimated to be $E_v = (2.25 \pm 0.05)$ eV.

Another group of researchers (Hull et al. [17]) initially assumed that the activation energy of dislocation propagation in the solid solution Ge_xSi_{1-x}/Si(100) depends on x and varies between 2.2 and 1.6 eV, the activation energies for silicon and germanium, respectively, determined earlier for bulk samples. Then

$$E_v(x) = (2.2 - 0.6x) \text{ eV} \tag{17}$$

and

$$V_{\text{d}} = V_0 \tau_{\text{eff}}^m \exp\left(-\frac{E_v - 0.6x}{kT}\right). \tag{18}$$

Measurements of dislocation velocity have been carried out directly in a transmission electron microscope (*in situ*, recorded on a video camera) and have been described in detail by Stach et al. [29]. Figure 5 depicts the overall results of measurements of the TD velocity made by these researchers [19]. In order to match the data the researchers introduced the velocity V^* normalized to τ_{eff} and x:

$$V^* = \frac{V_{\text{d}}}{\tau_{\text{eff}}} \exp\left(-\frac{0.6x}{kT}\right). \tag{19}$$

Note that although these researchers agree that the exponent m in expression (18) differs from unity, they nevertheless normalize the velocity of threading dislocations to τ_{eff} raised to the first power, which may introduce an error in determining the activation energy in layers with large values of τ_{eff}.

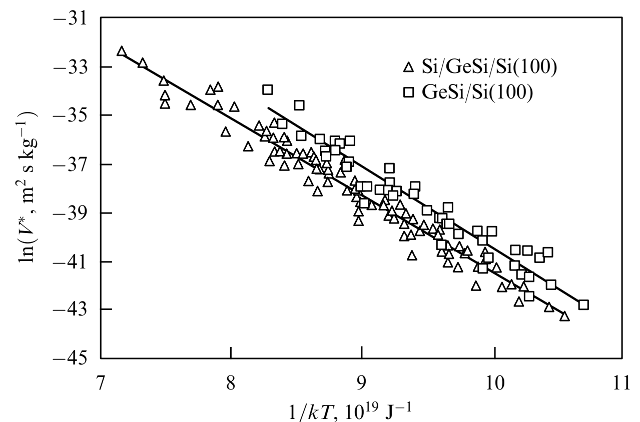

Figure 5. Normalized glide velocities of dislocations in the Ge – Si heterostructure measured directly during layer annealing in an electron microscope according to the data of Hull et al. [19].

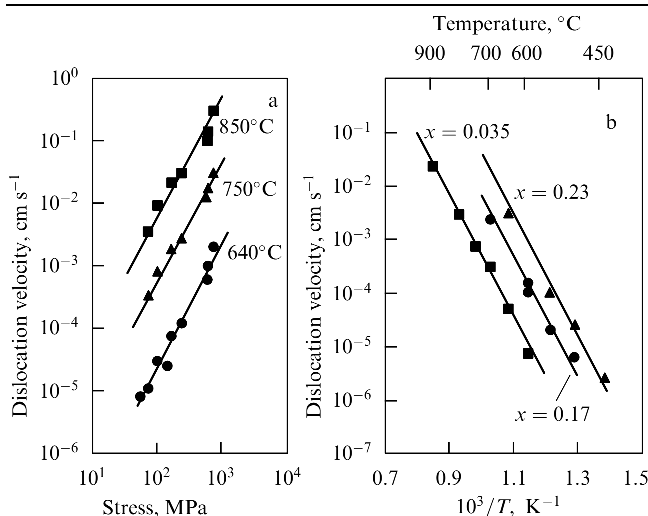

Figure 4. Dependence of the velocity of the propagation of 60° dislocations in strained Ge – Si layers on (a) stress and (b) reciprocal temperature according to Houghton [20].

Figure 6a summarizes the results of measurements of the activation energies for propagation of TDs made by Hull et al. [17]. The same figure depicts Houghton's data (the way in which these data were obtained has been described above). Clearly, there is a substantial difference between these two sets of data. Nevertheless, in our further discussion we will assume that the activation energy of TD propagation in stressed Ge_xSi_{1-x} layers on silicon with x up to 0.3 is close to 2 eV.

As is known, the universally accepted model of dislocation propagation is that based on the formation of double [15] and single kinks in dislocations. Due to thermal fluctuation or the presence of stresses, a double kink (DK) can form on a dislocation line (Fig. 6b). After a double kink has reached its critical size, it dissociates into two single kinks (SK), which move in opposite directions (Fig. 6b), which finally leads to a situation in which the dislocation line moves to the neighbor-

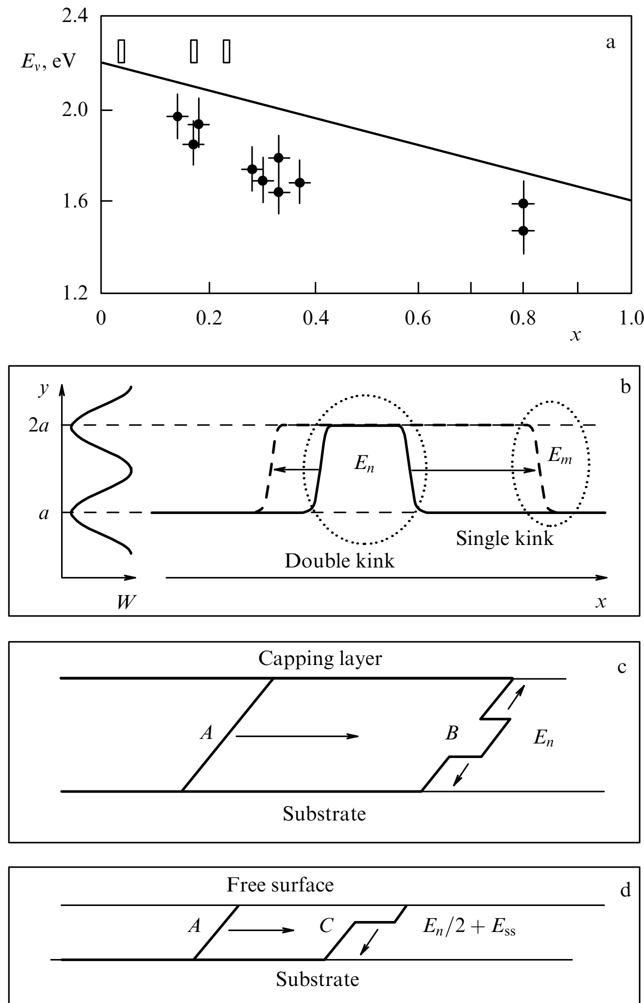

Figure 6. (a) Activation energy of dislocation propagation in the Ge–Si heterostructure according to Hull et al. [17] (crosses) and Houghton [20] (rectangles). (b)–(d) Diagrams illustrating dislocation propagation. (b) To the left, the potential relief showing two close energy valleys where dislocations could occur; to the right, the solid line represents a dislocation, and the dashed oval lines represent a double kink that was formed (activation energy E_n) and one of the single kinks moving in the directions indicated by arrows (activation energy E_m). (c) Dislocation propagation via the formation of a double kink. (d) Dislocation propagation via the nucleation of a single kink at the surface of a thin layer (activation energy $E_n/2 + E_{ss}$).

ing valley of the energy relief. It is assumed that such a mechanism of nucleation of double kinks with an activation energy E_n followed by recession of single kinks with an activation energy E_m occurs in massive samples and buried layers [30] (Fig. 6c). Thus, the activation energy of dislocation propagation discussed earlier consists of two parts: $E_v = E_n + E_m$. If the layer is thin, a single kink may form on the dislocation line at the surface, as shown in Fig. 6d. In this case the activation energy of SK formation is $E_n/2$ and of the energy of the kink that forms at the surface, E_{ss}. Since the latter is low, $E_n/2 + E_{ss} < E_n$. According to Hull et al., it is the higher probability of SK formation in layers with a free surface that explains the higher TD velocity in GeSi/Si layers compared to that in Si/GeSi/Si (all other things being equal), which is clearly demonstrated by Fig. 5.

All these data refer to dislocation propagation via gliding, i.e., to 60° dislocations, which are the most wide-spread dislocations in this system and which are the main participants in the plastic relaxation of strained GeSi layers on Si. Analysis of the data shows that the TD velocities in strained layers at temperatures above 450 °C (e.g., see Fig. 4) are in the 10-to-100-nm s^{-1} range. These values are large enough for dislocation propagation not to be the limiting factor forestalling the beginning of plastic relaxation in pseudomorphic layers that are in the metastable state and whose thickness is of the same order of magnitude. What is the limiting factor is the nucleation of misfit dislocations.

2.4 Propagation of misfit dislocations in strained epilayers. Theory and experiment

The nucleation of a dislocation loop in a strained layer is similar to the nucleation of a new phase (e.g., the emergence of a nucleus of the solid phase in a supercooled liquid) and requires that some amount of energy be spent. According to Matthews et al. [31], the energy of a dislocation loop of radius R is given by the formula

$$W_l = Gb^2 R \, \frac{2-\nu}{4(1-\nu)} \left(\ln \frac{\beta R}{b} + 1 \right) . \tag{20}$$

The gain caused by the decrease in the stresses during the formation of such a loop inside a strained layer is

$$W_s = 2\pi R^2 S \, \frac{G(1+\nu)}{1-\nu} \, bf . \tag{21}$$

Clearly, the additional energy of the emerging dislocation loop is proportional to the loop radius, while the decrease in the energy of the stresses accompanying the loop formation is proportional to the square of the loop radius. Accordingly, the algebraic sum of these energies as a function of R must have a maximum, as shown in Fig. 7a. This maximum is the energy barrier that can be overcome when, as a result of fluctuations, the dislocation loop reaches its critical radius R_c (Fig. 7a).

Figure 7a depicts the dependence of W_s, W_l, and $W_s + W_l$ on the radius of the dislocation loop when the concentration of Ge in the layer is 0.3. It is seen that the calculated energy barrier needed for the formation of such a loop, W_c, amounts to 250 eV and is much larger than the value ~ 2 eV [32] needed for the formation of a misfit dislocation with the observed density (on the order of several units per micron). More exact calculations that allow for the type of dislocation, the energy of the kink that forms at the surface of the layer when the dislocation half-loop passes through the bulk of the layer, and different values of the dislocation core parameter β [33, 34] yield somewhat smaller values of W_c, which nevertheless are close to or exceed 100 eV for a concentration $x \leqslant 0.3$ of Ge in the GeSi solid solution, which is apparent from Fig. 7b. Such calculations have led to the conclusion that homogeneous nucleation of misfit dislocations in pseudomorphic Ge_xSi_{1-x} layers with x up to 0.5 is impossible [33]. Nevertheless, misfit dislocations do appear in such heterostructures, and below we discuss in detail the various contemporary models and experimental observations of the initial stages in the relaxation of strained layers and the possible sources of misfit dislocations.

Eaglesham et al. [33] and Hull and Bean [34] (the curves in Fig. 7b have been taken from these papers) call the energy barrier needed for the formation of a dislocation loop of critical radius the activation energy or the activation barrier. This barrier, as Fig. 7b clearly shows, depends on x, i.e., on

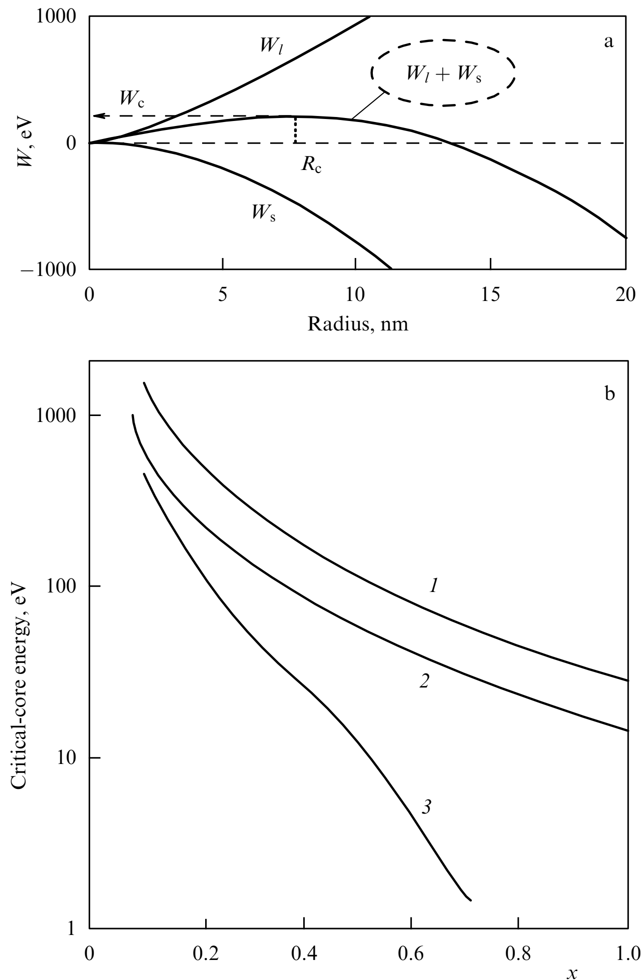

Figure 7. (a) Example of calculations that should be performed in order to determine the critical radius of a dislocation loop and the loop's formation energy for $Ge_{0.3}Si_{0.7}$/Si(001). (b) The size of the barrier for the appearance of a dislocation loop of critical radius according to Hull and Bean [34] (curves *1* and *3*) and Eaglesham [33] et al. (curves *1* and *2* for 60° dislocations and curve *3* for 90° dislocations).

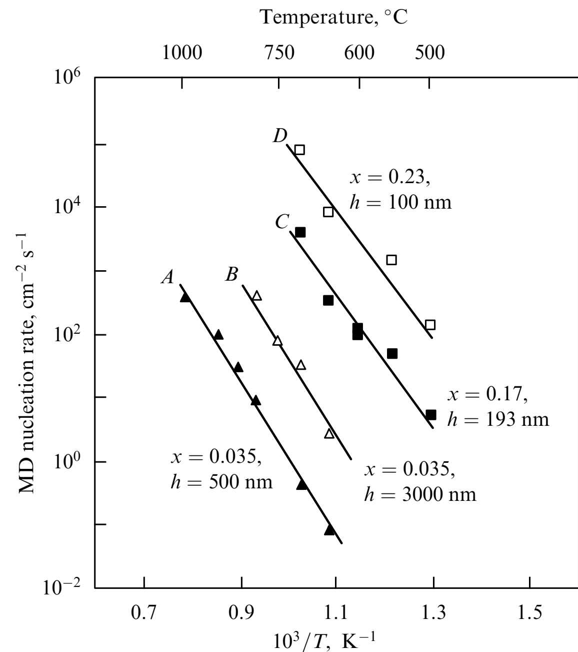

Figure 8. MD nucleation rate as a function of the reciprocal temperature according to Houghton's data [20].

the size of the stresses ε. Mooney et al. [35], who calculated the value of this energy by the method discussed at the beginning of this section, gave the following formula: $W_c = K/\varepsilon$ (here K is a constant), which qualitatively reflects the pattern in Fig. 7b. According to this formula, the activation energy needed for dislocation-loop nucleation is inversely proportional to the stresses in the layer. At the same time, the physical idea on which the notion of the activation energy of a process is based amounts to the following: there is a minimum energy characterizing the activation nature of the process; this energy can usually be found from the slope of the curve representing the temperature dependence of a reliably measurable parameter (the curve is plotted in Arrhenius coordinates).

In the same extensive paper (Ref. [20]), Houghton approached the problem of MD nucleation from a different angle. In the previous section, we briefly discussed his method of estimating the nucleation rate. First, the measured values of the MD nucleation rate were placed in the ($\ln(\mathrm{d}N/\mathrm{d}t)$, $1/T$) plane, and then the curves depicted in Fig. 8 were built. Clearly, the slopes of these curves are practically the same, and the nucleation activation energy W_n extracted from the value of this slope is 2.5 ± 0.5eV and is independent of x and τ_{eff}. On the basis of these results, Houghton derived a semiempirical expression for the MD nucleation rate

$$\frac{\mathrm{d}N(t)}{\mathrm{d}t} = N_0 \tau_{\mathrm{eff}}^n \exp\left(-\frac{W_n}{kT}\right), \tag{22}$$

which formally is similar to the expression (16) for the velocity of dislocation propagation in strained layers. Here, τ_{eff} is the same effective stress as in (16), and N_0 is an adjustable parameter, which, Houghton believes, is the initial density of the points of most probable nucleation of misfit dislocations, which is different for different Si substrates. The exponent n determined from the experimental data is equal to 2.5.

Thus, according to one model, the height of the energy barrier needed for MD nucleation depends on the mismatch between the lattice parameters of the layer and the substrate as $1/\varepsilon$, where $\varepsilon \sim f$, while according to the other model, the activation energy of MD nucleation is close to 2.5 eV and is independent of x. This contradiction can be resolved by assuming that there is a certain structure consisting of the minimum possible number of atoms that is a dislocation nucleus, different for each type of dislocation in a given material. For such a nucleus to appear in an initially perfect crystal matrix, an energy barrier (precisely, the one that Houghton [20] determined in his experiments for Ge_xSi_{1-x} compositions with x up to roughly 0.3) must be surmounted. The physical mechanism by which the layer thickness affects the rate of MD nucleation has yet to be established. Equation (22) shows that the MD nucleation rate $\mathrm{d}N/\mathrm{d}T$ is proportional to τ_{eff} raised to the power of 2.5, while $\tau_{\mathrm{eff}} \sim h$ [Eqn (14)]. There are two possibilities here: (a) the MD nucleation centers are (to the first approximation) located uniformly within the bulk of the layer, and the number of centers increases as the layer becomes thicker (e.g., see Ref. [33]); (b) an MD loop or half-loop (the minimum possible nucleus that requires the energy barrier W_n to be surmounted) that has nucleated at the interface (where supposedly most centers are

located) or at the surface passes, via fluctuations, through the entire thickness of the layer, after which the force F_c proportional to the layer thickness [Eqn (9)] comes into play and moves the threading branches in opposite directions (or, if the layer is thin, the dislocation loop is annihilated).

Nevertheless, many observations of plastic relaxation in strained GeSi layers did not lead to a clear understanding of the reasons for, and sources of, misfit dislocations. Beanland [36] pointed out the presence of two waves of plastic relaxation formation in a strained layer: the first wave is generated at small layer thicknesses by primary sources, while the second develops due to secondary sources, which are related to different variants of dislocation multiplication. Vdovin [37] lists examples of models of primary sources of MD nucleation found in the literature. The examples can be broken down into four groups: (a) the bending of dislocations that grow from the substrate, (b) the nucleation of dislocation half-loops at the surface of the layer, (c) various internal imperfections that serve as sources of heterogeneous nucleation of misfit dislocations (such as coherent particles of β-SiC at the substrate surface, which may serve as a source of a threading dislocation and then of a misfit dislocation [27]), and (d) the so-called rhombic structures discovered by Eaglesham et al. [33] in the bulk of GeSi. Note that all attempts to identify these structures in group (d) to inhomogeneities that are the primary reason for the formation of rhombic sources have failed. Perovic and Houghton [21] proposed using composition microinhomogeneities in the GeSi solid solution as an internal source (certain clusters that generate a dislocation loop). Hull and Bean [34] point out the possible capability of the GeSi solid solution to modify the local structure near the dislocation core when the Ge and Si atoms become shifted, which may lead to a substantial decrease in the stresses at this point and a decrease in the energy of the deformed core. The latter factor in turn lowers the energy of dislocation loop formation.

In the case of growth on silicon substrates, we can ignore sources of the first type (the bending of dislocations that grow from the substrate) due to the high quality of such substrates: $N_d < 10^2$ cm^{-2}. The nucleation of dislocation half-loops at the surface of a strained layer has been the most popular mechanism among the researchers for the last twenty years (e.g., see the reviews of Fitzgerald [6] and Jain et al. [38]). However, by the end of the 1980s, some researchers found that the nucleation of such half-loops is unlikely to occur on the smooth surface of a growing layer due to the high energy barrier (amounting to tens of electronvolts [1, 33], a fact we mentioned earlier).

The surface of a strained layer may become rough during growth of the layer in accordance with the elastic relaxation mechanism developed primarily in connection with the new avenue of research in heteroepitaxy of highly strained structures: nanometer-scale islands of Ge on Si and of InAs on GaAs [39, 40]. On such a surface, due to the geometric increase in stresses on inhomogeneities, the barrier for MD formation becomes lower. The researchers found that such a mechanism may indeed be responsible for MD injection from the surface; however, the efficiency of this mechanism manifests itself in experiments with systems in which the average mismatch of the lattice parameters is roughly 1% or more [41, 42]. The range of strains for which the growing surface loses its morphological stability even before plastic relaxation has begun narrows with increasing temperature due to the increase in the surface diffusion of the adatoms. Accordingly, various methods that facilitate two-dimensional growth, such as cooling to low temperatures and reducing the deposition rate in combination with the *in situ* control of the planarity of the surface, make it possible to move the limit of morphological stability into the region of more strained compositions of GeSi solid solutions and to exclude the effect of the surface on the plastic relaxation of epilayers. Nevertheless, misfit dislocations are surely to emerge in the growth and annealing of multilayer heterostructures and in so-called buried GeSi layers, i.e., strained layers covered by a capping layer of Si. In this case the model in which the surface of the strain layer becomes rough does not operate, since the capping layer is not strained. In multilayer strained heterostructures subjected to annealing for the purpose of observing relaxation processes, misfit dislocations are observed primarily at the interface with the substrate. Thus, one can conclude that the role that the surface plays in MD nucleation in layers with average and small mismatches of the lattice parameters ($\sim 1\%$ or less) has been exaggerated in the last few years. Nevertheless, it has been firmly established that the internal sources of MD nucleation described above play the leading role at the initial stages of plastic relaxation of GeSi solid solutions.

2.5 Plastic relaxation of epilayers

2.5.1 The classical approach and the experimental deviations. In quasi-equilibrium conditions and in the absence of barriers, the formation of misfit dislocations begins when the thickness of the pseudomorphic layer exceeds h_c. The stresses in the layer diminish and the critical thickness increases. For the formation of a new portion of misfit dislocations, this new critical thickness must again be exceeded. Thus, the layer gradually and plastically relaxes as it becomes thicker. The residual elastic strains can be expressed as follows:

$$\varepsilon(t) = f - b_{\text{eff}}\rho(t)\,, \tag{23}$$

where b_{eff} is the projection of the Burgers vector on a normal that lies in the interface plane and is perpendicular to the line of intersection of the glide plane and the interface plane, $\rho(t)$ is the linear density of the dislocations, and, according to Hu [43],

$$\varepsilon(t) = f\,\frac{h_c}{h(t)} \quad \text{at} \quad h \geqslant h_c\,. \tag{24}$$

In Fig. 9a this dependence is depicted by the solid curve. As noted earlier, in many cases the value of the theoretical critical thickness is exceeded (see Fig. 3). Two critical thicknesses can be introduced here: the theoretical, or equilibrium, critical thickness h_c, and the experimental critical thickness h_c^{exp}. The fact that these two quantities are always different does not mean that Matthews's calculations are incorrect — simply in growing semiconductor layers the barriers of various kinds play an important role: they hinder the injection of misfit dislocations. Special studies conducted by Houghton et al. [10] that involved $Ge_xSi_{1-x}/Si(001)$ solid solutions with $x = 1 - 15\%$ show an 'excellent' (as the researchers write) fit of the results of Matthews's calculations to the experimental results. This also becomes evident from Fig. 3 for epilayers grown or annealed at high temperatures. Matthews's equilibrium models used to determine the critical thickness for MD injection define a fundamental parameter

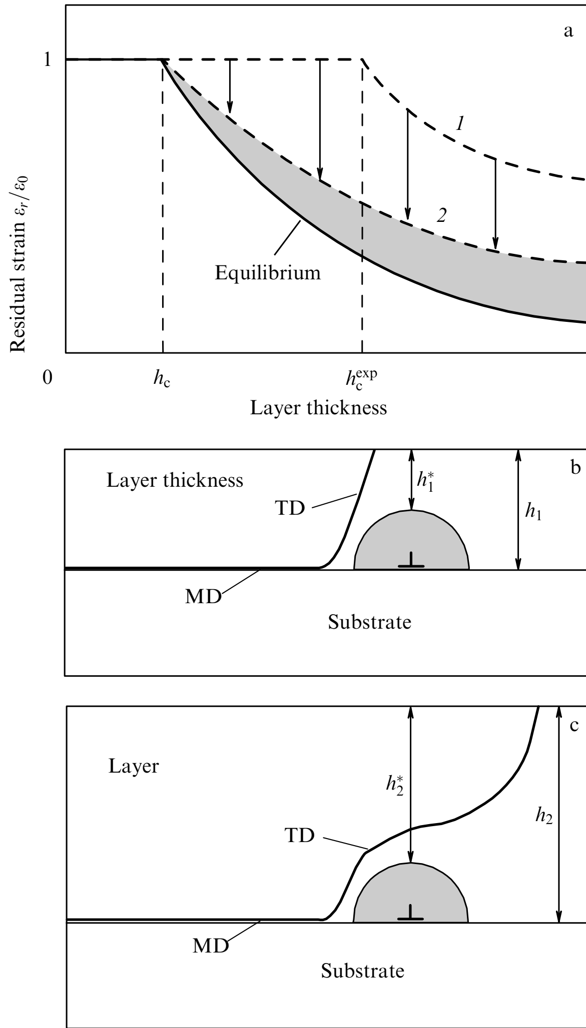

Figure 9. (a) Schematic of the dependence of the plastic relaxation of strained layers on the layer thickness. (b) and (c) Blocking of a propagating TD that encounters an orthogonally positioned misfit dislocation.

h_c, which depends on the specific pair of materials forming the heterostructure, the mismatch, and the type of crystallographic plane of the interface. Many researchers use this parameter as a certain limit in thickness below which a pseudomorphic epilayer is stable, i.e., is not influenced by MD injection, while above this limit the layers is in a metastable state. The tendency of pseudomorphic layer within this region near this limit to form MDs (which then propagate), i.e., the beginning and rate of plastic relaxation depend on two new parameters: the temperature and the time that the heterostructure stays at this temperature (Fig. 9a, curve *1*). Accordingly, h_c^{exp} for a specific heterostructure is a floating quantity depending on these new parameters. In order to eliminate the 'dormancy' of plastic relaxation of pseudomorphic layers, one must either grow the layers using small rates (which not always leads to the necessary result) or anneal the layer at elevated temperatures after growth. Nevertheless, as the vast body of data from the literature suggests, an equilibrium experimental dependence of the plastic relaxation of a heterostructure approaches the theoretical dependence but does not coincide with it (Fig. 9a, curve *2*).

2.5.2 Models of kinetic damping of plastic relaxation. Matthews et al. [44] were the first to introduce a velocity dependence of the friction force acting on a propagating dislocation into the force-balance model. Dodson and Tsao expanded Matthews's ideas by introducing a velocity dependence of dislocation multiplication. Fox and Jesser [46, 47] developed the concept of additional forces acting on a dislocation in a strained layer in greater detail.

Let us go back to Section 1.3 and Eqn (14), which implies that the dislocation propagation velocity is proportional to τ_{eff} raised to power m (the so-called effective stress). When τ_{eff} vanishes, the conditions in the layer reach those that exist at critical thickness. For a layer that is in a metastable state ($h > h_c$), $\tau_{eff} > 0$ and, on the assumption that $m = 1$ (to simplify matters), combining (14) and (16) and multiplying the result by bh, we get

$$S\,\frac{2G(1+\nu)}{1-\nu}\,\varepsilon(bh) = \frac{Gb(1-\nu\cos^2\alpha)\cos\phi}{4\pi h(1-\nu)} \times \left(\ln\frac{\beta h}{b}+1\right)bh + \frac{V_d}{V_0}\exp\left(\frac{E_v}{kT}\right)bh\,, \quad (25)$$

or $F_c = F_l + F_v$, where F_v is the friction force (according to Fox and Jesser [46], $F_v = BhV_d\exp(Q_i/kT)$, and B is a constant) related to the energy of the dissipation processes that accompany the propagation of dislocations.

The velocities of dislocation propagation discussed in Section 1.3 were measured at the initial stages of layer relaxation, so that the interaction between dislocations was rightly ignored. Accordingly, the activation energy of dislocation propagation, calculated by Houghton [20] and Hull et al. [17], was found to be in the 1.5 – 2.2-eV range. Several values of the dislocation propagation velocity found in experiments were so large that the researchers were prompted to assume that the initial stage of plastic relaxation is not limited by the propagation of dislocations in pseudomorphic GeSi/Si layers at the commonly used growth temperatures (400 – 600 °C), and the more so at higher annealing temperatures. However, in the process of deeper relaxation (the second wave, according to Beanland [36]), the slowing-down of TD propagation and the blocking of these dislocations may be due to their interaction. As the fraction of plastic relaxation of a layer of fixed thickness decreases, the driving force of relaxation (τ_{eff}) and the TD propagation velocity become smaller. The latter also decreases because the activation barrier for dislocation propagation becomes higher, and the barrier can be said to become effective (Q_i in the works of Fox and Jesser [46, 47]); apparently, the height of this barrier can be much larger than E_v, which is a quantity determined from experiments.

Hull and Bean [48] concretized the mechanism of drag on the TD propagation in layers for which a network of misfit dislocations has already been formed at the interface with the substrate. Figure 9b depicts a diagram that helps to explain the interaction of two dislocations: a TD branch propagating to the right, and a misfit dislocation that is orthogonal to this branch and lies in its way. This misfit dislocation forms a strain field (the hatched semicircle) that inhibits the TD propagation. According to Hull and Bean [48], the analog of equation (25) in this case is $F_c = F_l + F_{dp}$, where F_{dp} is the dragging force caused by the interaction of the propagating TD branch and the orthogonal MD network.

2.5.3 Force-balance models with additional damping forces. A somewhat different interpretation of TD damping on an orthogonal MD network has been given by Gillard, Nix, and Freund (GNF) [49]. Figure 9b illustrates the fact that the effective thickness h_1^* of a layer above a misfit dislocation lying in the interface plane is smaller than the total layer thickness. The value of h_1^* can prove to be smaller than the critical thickness, with the result that the TD is stopped. When the layer becomes thicker (Fig. 9c), the effective thickness increases (h_2^*) and the TD bends and continues its propagation. Thus, the equilibrium MD density at which the effective stress forcing the TD to move vanishes [see Eqn (15)] is lower for a layer of thickness h due to the fact that $h^* < h$. The greater the mismatch between the lattice parameters of layers and substrate (and hence the thinner the layers when the MD network is formed), the stronger the effect — a situation actually observed in experiments (e.g., see Ref. [48]).

One of the authors of the GNF model (Freund) showed (see Ref. [50]) that for threading dislocations gliding along an inclined plane and interacting with a straight 60° misfit dislocation, only four of the eight combinations of the Burgers vectors are independent. Hence, four variants of the dependence of the residual elastic strain on the layer thickness have been calculated. The authors of the GNF model introduced what became known as the blocking potential of an orthogonal MD network, whose stress field is calculated with allowance for the edge and screw components of 60° misfit dislocations. Figure 10 depicts the dependence of the residual elastic strain in the $Ge_{0.3}Si_{0.7}/Si(001)$ layer on the layer thickness calculated using the equilibrium Hu model [43] [see Eqn (23)]. The same figure depicts the theoretical curves of the GNF model for $x = 0.35$ (the hatched region represents the dependence range for the four combinations of the Burgers vectors). The experimental points have been taken from the paper by Gillard et al. [49] and from Ref. [14]. Clearly, on the whole the calculated curves of the GNF model agree with the experimental data, but systematically the latter are above the curves. The researchers note that there are additional factors that have not been taken into account but hinder the penetration of MD branches and thus limit still further the degree of plastic relaxation in strained epilayers (e.g., the blocking at surface imperfections [51]).

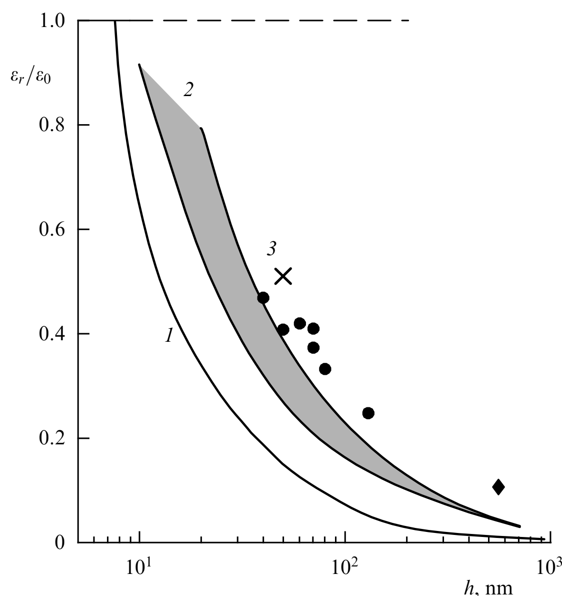

Figure 10. Residual elastic strain in Ge – Si layers as a function of the layer thickness. Curve *1* represents the results of calculations for the classical variant with $x = 0.3$ done by Hu [43], curve *2* represents the theoretical results of Gillard et al. [49] with $x = 0.35$, and curve *3* represents the results of calculations done by Fisher et al. [52] with $x = 0.3$. The experimental points have been taken from Refs. [49] (solid circles) and [14] (the lozenge).

Fisher [7, 52] tackled this problem from another angle. The resolved shear stress acting on a 60° threading dislocation during plastic relaxation of a layer can be expressed as follows:

$$\tau(f - \delta) = S\,\frac{2G(1+\nu)}{(1-\nu)}\left(f - \frac{b}{2p}\right), \tag{26}$$

where $b/2p = \delta$ is a factor that diminishes the initial elastic strain due to plastic relaxation, and p is the average distance between dislocations. [The expression $f = b/2p$ can be used to determine the minimum distance between misfit dislocations that corresponds to complete plastic relaxation of the layer; e.g., $p = 16$ nm for $x = 0.3$. See also Eqns (4) and (23)]. As an additional counteracting factor, Fisher introduces an internal stress generated by a misfit dislocation lying in the interface plane. The resolved internal shear stress recalculated with respect to the glide plane for 60° threading dislocations with an average distance p between them can be expressed as follows:

$$\tau_{\mathrm{MD}} = \frac{Gb(1-\nu/4)}{2\pi p(1-\nu)}\ln\frac{p}{2b}\,. \tag{27}$$

If this counteracting factor is taken into account in (26), the total resolved shear stress $\tau^* = \tau(f-\delta) - \tau_{\mathrm{MD}}$ is given by the formula

$$\tau^* = S\,\frac{2G(1+\nu)}{1-\nu}\left[f - \frac{b}{2p}(1-A)\right], \tag{28}$$

where

$$A = \frac{1-\nu/4}{2\pi\cos\lambda(1+\nu)}\ln\frac{p}{2b} \tag{29}$$

is a factor that additionally reduces the resolved shear stress depending on the current MD density. As a result of such hardening, certain residual elastic strains are retained in the GeSi/Si layer after the thermal process of plastic relaxation has been carried out, and this state is stable. The symbol $\times$ in Fig. 10 denotes the calculated point of such a stable state of a 50-nm thick $Ge_xSi_{1-x}/Si(001)$ layer with $x = 0.3$ [52].

2.6 Interaction of dislocations and multiplication. Secondary sources of misfit dislocations

Once misfit dislocations have appeared, they can multiply via interaction. Vdovin [37] examined the main secondary sources arising from the interaction of the dislocations present in a strained layer. Two such sources are the most popular: a source based on the mechanism proposed by Hagen and Strunk [53], and the Frank – Read source [15]. The Hagen – Strunk mechanism operates in thin layers, since here the branches of a split misfit dislocation are supposed to have emerged at the surface. A configuration of dislocations corresponding to this mechanism was observed by Vdovin [37] and Rajan and Denhoff [54] in GeSi/Si(001) epilayers.

However, Eaglesham et al. [33] doubted the effectiveness of the Hagen – Strunk mechanism and assumed that such a configuration may also correspond to other mechanisms of dislocation multiplication. Vdovin [55] assumes that the Hagen – Strunk mechanism can operate mainly in thin strained layers for which the difference in the lattice parameters of the layer and the substrate is small.

For the Frank – Read mechanism to operate, the layer thickness must substantially exceed the critical value [56]. The formation of a new dislocation loop is related to the pinning of a threading dislocation inside the strained layer. Mooney et al. [35] and LeGoues et al. [57, 58] studied the source in strained GeSi/Si(001) layers that operated on intersecting glide planes (111). They called this source a modified Frank – Read (MFR) source. A characteristic feature of this mechanism is the deep penetration of dislocations into the substrate.

Three years after Eaglesham's paper [33], Capano [59] also doubted the effectiveness of the Hagen – Strunk mechanism and proposed a new variant of MD multiplication that leads to the same experimental result — the appearance of bundles of 60° misfit dislocations with the same Burgers vector. The new mechanism postulates the emergence of sequential Frank – Read sources during the propagation of a threading dislocation. Capano [59] corroborates this mechanism by examples based on experimental data. The quasi-periodic blocking of a propagating TD cannot be explained by the presence of an imperfection in its path, so Capano explained it by TD 'pulsations', i.e., quasi-regular constriction of the dissociated propagating TD.

As noted by Beanland [56], for secondary sources of misfit dislocations to operate, the layers must be thick. He introduced a new critical thickness, at which it becomes possible for a strained layer to produce secondary sources. To illustrate this, in Fig. 11 we depict the dependence, calculated by Beanland, of the critical thickness needed for a Frank – Read source to begin operating, on the mismatch of the lattice parameters. Clearly, this new critical thickness greatly exceeds h_c calculated according to Matthews's method for the beginning of MD injection. The inset in Fig. 11 shows the experimental estimates of Capano [59] and Tuppen et al. [60] for the layer thickness upon reaching which the multiplication of dislocations in $Ge_xSi_{1-x}/Si(001)$ layers with $x = 0.13$ becomes observable. Clearly, these thicknesses exceed h_c by a factor of ten. Thus, plastic relaxation of strained layers proceeds in two stages. First, the primary sources of misfit dislocations come into play. It can be assumed that the purer and the more perfect the pseudomorphic layer is, the smaller the number of such sources. Prolonged annealing of such thin layers, which are in a metastable state but do not exceed, in thickness, the threshold for the start-up of secondary sources, does not lead to the desired result, i.e., deep plastic relaxation. And only when the growing layer reaches a certain thickness does the possibility of MD multiplication and further plastic relaxation emerge.

Another feature of plastic relaxation of GeSi/Si layers is connected with the two types of MDs that are most common in such a material: 60° and 90° dislocations. As noted earlier, the 90° MDs are energetically more favorable than 60° misfit dislocations, but they are sessile. For this reason, their entry into a strained layer is much more difficult. As x gets larger and as the layers undergo prolonged annealing, the fraction of 90° misfit dislocations becomes greater [61]. The type of misfit dislocation is established with a transmission electron microscope (TEM) with a picture of the same section being taken twice. If the diffraction vector **g** proves to be parallel to an edge dislocation line, i.e., perpendicular to the dislocation's Burgers vector, such a dislocation cannot be seen on a TEM image.

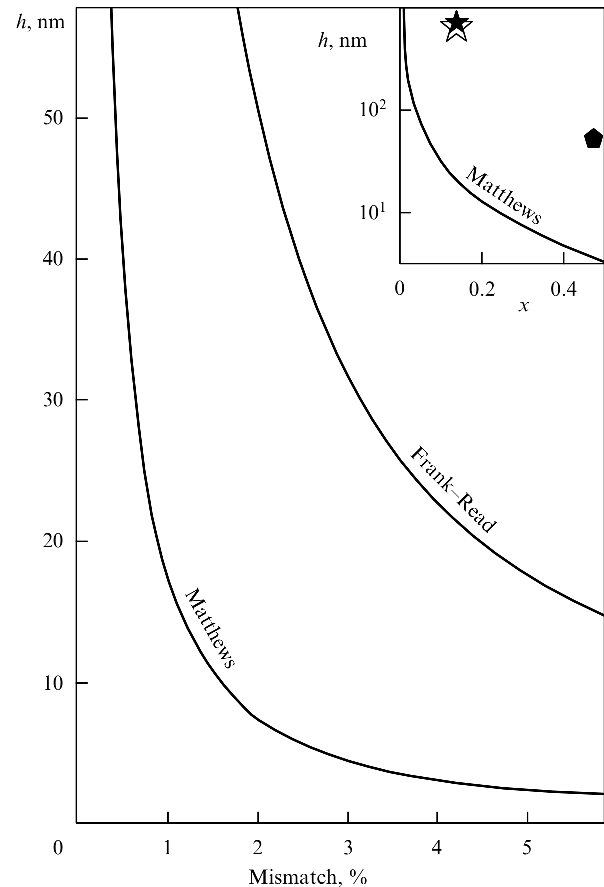

Figure 11. Calculated (Beanland [56]) critical thickness needed for a Frank – Read source to begin operating compared to the calculated (Matthews) critical thickness for MD injection, as functions of the mismatch between the lattice parameters of layer and substrate. The inset depicts the critical thickness as a function of x for solid Ge_xSi_{1-x} solutions; the solid pentagon indicates a calculated point taken from the main dependence of a heterostructure thickness at which a Frank – Read source begins to operate, and the stars are the experimental points taken from the works of Capano [59] and Tuppen et al. [60] (according to the researchers, they correspond to the beginning of MD multiplication in the solid solution $Ge_xSi_{1-x}/Si(001)$ with $x = 0.18$).

Figure 12 depicts an example of the dislocation structure of a $Ge_{0.3}Si_{0.7}/Si(001)$ layer annealed at 800 °C. The two dark-field images of the same section (Figs 12a and 12b, respectively) obtained under conditions of two-wave diffraction from mutually perpendicular families of {220} planes illustrate the complete extinction of purely edge Lomer misfit dislocations when $\mathbf{g} \times \mathbf{b} = 0$. On the complementary parts of Fig. 12 such dislocations are designated by short arrows.

There are several models explaining the generation of 90° misfit dislocations in relaxed layers. At large mismatches, at x close to 1, a strained layer in the initial stage of growth is transformed into an island layer, and the large fraction of 90° misfit dislocations (up to 100%) can be explained by the fact that these dislocations are generated at the edges of the islands. However, this case is not representative when strained layers of solid solutions GeSi/Si are grown, since in

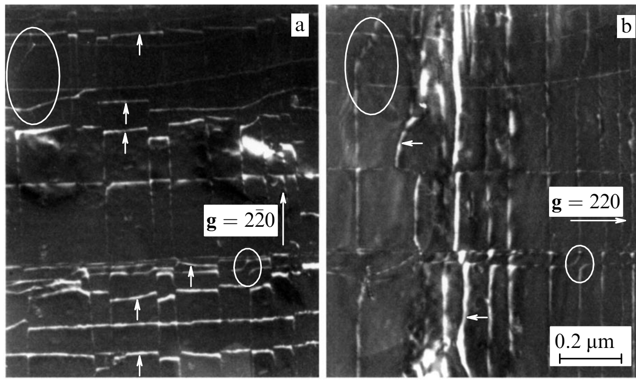

Figure 12. Example of identification of 90° misfit dislocations. The ovals designate the specially selected regions, identical on both micrographs. The pictures have been provided by A K Gutakovskiĭ.

the MBE method of growing epilayers there has long been a tendency toward planarization of the growing surface (low temperatures and growth rates, and the use of surface-active substances, e.g., antimony [62]). Nevertheless, 90° misfit dislocations are observed over the entire composition spectrum of GeSi/Si layers. According to Eaglesham's paper [33] and a more detailed paper by Vdovin [63], the generation of L dislocations may be due to the interaction of neighboring parallel 60° misfit dislocations with the appropriate Burgers vectors in accordance with the reaction

$$a/2[101] + a/2[01\bar{1}] = a/2[110]\,. \tag{30}$$

Here, the neighboring 60° misfit dislocations or their separate branches either rise to the layer or sink to the substrate along inclined glide planes until they all merge. Such configurations have been observed in experiments (see Ref. [63]). Gosling [64] has shown, by theoretical reasoning, that the act of nucleation of a loop with a 60° misfit dislocation at the interface in a region where a 60° misfit dislocation already exists (with subsequent transformation into a Lomer misfit dislocation) has a much lower energy barrier than the act of nucleation of a single loop. Finally, Kvam et al. [1] proposed a variant of nucleation of a complementary 60° dislocation at the surface of a thin layer under the effect of the stress field of a 60° misfit dislocation present at the interface.

2.7 Buried epilayers and multilayer heterostructures. Special features of plastic relaxation

Along with single-layer strained heterostructures, strained-layer superlattices (SLSs) consisting of several dozen layers of strained GeSi solid solution separated by barrier layers of silicon have been attracting more and more attention. The use of barrier layers has a twofold purpose. During the growth process, such a layer smooths the surface of the heterostructure after the deposition of each strained layer [65]. But its structural purpose, so to say, is to decrease the average strain in the heterostructure. The appearance of additional parameters of a multilayer heterostructure, such as the barrier layer thickness $h_{\rm b}$, the strain $\varepsilon_{\rm b}$ in a barrier, the number N of barrier pairs, and the thickness $h_{\rm cap}$ of the upper capping layer, leads to an increase in the number of degrees of freedom, which results in a greater variety of properties and a richer nature of relaxation of the heterostructure. On the other hand, this complicated the study and description of possible modes of plastic relaxation of such heterostructures.

A special case of strained-layer superlattices is what is known as compensated superlattices, in which the barrier layer is also under strain but of opposite sign. Here, by a thorough selection of the thicknesses of the barrier layers and the stresses in these layers, the average strain in such a heterostructure may be close to zero, which makes it possible to grow such multilayer heterostructures with a large number of layer pairs.

The strain averaged over the heterostructure (net strain) can generally be written as follows:

$$\bar{\varepsilon} = \frac{N(\varepsilon_{\rm f} h_{\rm f} + \varepsilon_{\rm b} h_{\rm b})}{N(h_{\rm f} + h_{\rm b}) + h_{\rm cap}}\,, \tag{31}$$

where $N(h_{\rm f} + h_{\rm b}) + h_{\rm cap} = H$ is the total heterostructure thickness. In most cases the thickness of each strained layer is smaller than the critical thickness for MD injection. As the number of layer pairs increases, the total thickness H of the heterostructure increases too, while the net strain remains practically constant [see Eqn (31)]. Such a heterostructure can be interpreted as being a quasi-homogeneous layer of thickness H with a strain $\bar{\varepsilon}$ in it that obeys the laws of plastic relaxation described above. As the overall thickness of the heterostructure increases, plastic relaxation begins, with MDs being injected at the heterostructure – substrate interface, while TDs penetrate the entire thickness of the heterostructure and exit at the surface, as shown in Fig. 13a. The threading branch of the dislocation is under an effective shear stress

$$\tau_{\rm eff}^{\rm SM} = S\,\frac{2G(1+\nu)}{(1-\nu)}\,|\bar{\varepsilon}| - \frac{Gb(1-\nu\cos^2\alpha)\cos\phi}{4\pi H(1-\nu)} \times \left(\ln\frac{\beta H}{b} + 1\right), \tag{32}$$

and the critical thickness for the injection of misfit dislocations is

$$H_{\rm c} = \frac{b(1-\nu\cos^2\alpha)}{8\pi|\bar{\varepsilon}|(1+\nu)\cos\lambda}\left(\ln\frac{\beta H_{\rm c}}{b} + 1\right). \tag{33}$$

Since the force acting on the dislocation is always positive, Eqns (32) and (33) contain the absolute value of the average strain.

By introducing a strain of opposite sign into the barrier layer, one can perfectly balance the strain in the main layer. Figure 14 depicts the dependences of the critical thickness expressed in the number of pairs of the main and barrier layers for a hypothetical heterostructure with the following parameters: the main layer is elastically compressed to $\varepsilon = 1\%$, and $h_{\rm f} = h_{\rm b} = 8$ nm (the thickness of the main layer is somewhat smaller than the critical thickness for a single layer with $\varepsilon = 1\%$; see Fig. 3). Clearly, the curve represents a resonance: the admissible number of pairs of layers increases as we get closer to perfect balance, and then decreases as overcompensation is achieved ($\varepsilon_{\rm b} > 1\%$).

The mechanism of relaxation of multilayer strained heterostructures in which misfit dislocations are injected at the substrate – heterostructure interface has indeed been observed [61]. We will call it mechanism A. The change in the stress distribution in such a relaxing heterostructure is depicted in Fig. 13c. Clearly, the stresses in the main part of the heterostructure are redistributed between the layers of the solid solution and the barrier layers, while the capping Si layer becomes stretched.

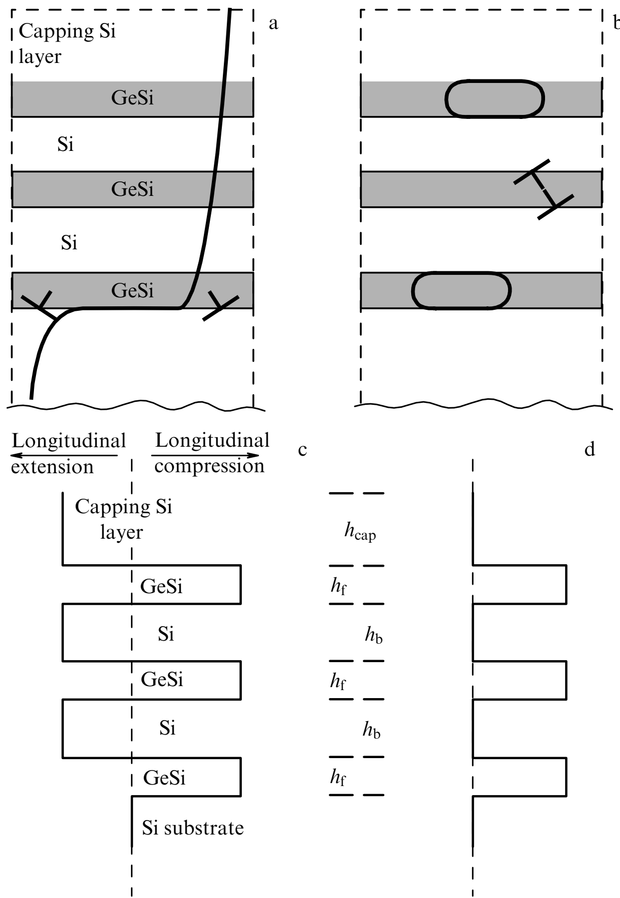

Figure 13. Two ways of injecting misfit dislocations in a heterostructure according to Houghton [61]: (a) at the heterostructure – substrate interface and (b) inside an individual layer. The stress distribution in such plastically relaxing heterostructures is schematically shown in (c) and (d), respectively. \

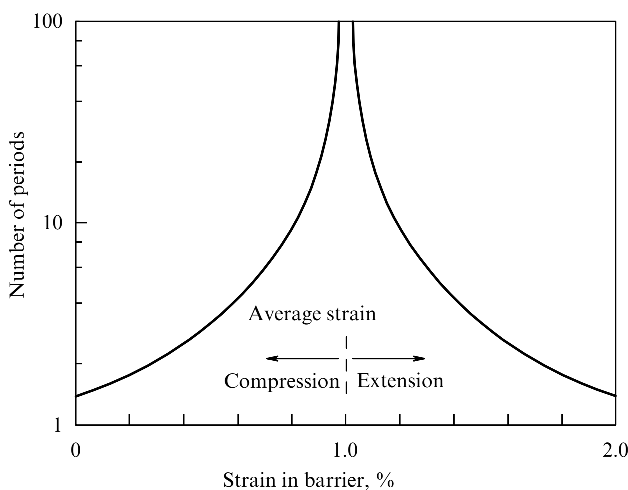

Figure 14. Structure stability of a multilayer heterostructure as a function of the strain in the barrier (the results of calculations).

Another possible variant of the relaxation of a strained heterostructure is depicted in Fig. 13b [61]. The lattice parameter mismatch is balanced by the misfit dislocations that form at the upper and lower boundaries of each layer, what is known as pair misfit dislocations, or dislocation dipoles, whose distinctive feature is that the upper and lower 60° dislocations are in the same glide plane but have oppositely directed Burgers vectors [66]. This relaxation mechanism (we call it mechanism B) operates when the thickness of each pseudomorphic layer begins to exceed the critical thickness for MD injection. In this case, each layer relaxes independently (Fig. 13d).

A special place in studies of relaxation of strained layers is occupied by what is known as buried layers, or heterostructures that consist of a strained layer of thickness h_f (e.g., a solid Ge – Si solution) and a capping layer of thickness h_{cap} that matches the substrate (e.g., Si). A capping layer deposited on a pseudomorphic layer and with a lattice parameter coinciding with that of the substrate increases the equilibrium critical thickness h_c for MD injection. For a semiinfinite capping layer, the value of the critical thickness doubles. This follows from simple logical arguments: if we take two identical pseudomorphic layers with thicknesses equal to the critical one, h_c, and place one atop the other, we get a buried layer of thickness $2h_c$ that is still in a structurally stable state.

Injecting a misfit dislocation in the form of a dipole into a buried layer is less advantageous in comparison to injecting single dislocations since during the propagation of the threading part of such a loop along a layer of thickness h_f the counteracting part of the effective shear stress [the right-hand side of Eqn (14)] doubles. However, when the relaxation of a buried layer proceeds according to mechanism A, i.e., via single dislocations, the threading part of the propagating dislocation exits at the surface of the capping layer, and its propagation through the layers of thicknesses h_f and h_{cap} is also hindered due to its forced motion in the unstrained part of the heterostructure, i.e., in the capping layer. Thus, depending on the thickness of the capping layer, different mechanisms of MD injection should play the leading role.

This problem has been studied in detail by Houghton et al. [20, 67]. By interpreting the energy of the interaction of a dislocation pair as the work that must be done so that a second dislocation is injected from the surface to the depth h_{cap},

$$E_i = \frac{Gb^2(1 - \nu\cos^2\alpha)}{2\pi(1-\nu)} \ln\frac{h_f}{h_f + h_{cap}}\,, \tag{34}$$

Houghton derived an expression for the effective shear stress for a propagating dislocation pair (the 'unity' under the logarithm sign is ignored):

$$\tau_{eff}^{DP} = S\,\frac{2G(1+\nu)}{(1-\nu)}\left[\varepsilon - \frac{b(1-\nu\cos^2\alpha)}{4\pi h_f(1+\nu)} \times \left(2\ln\frac{\beta h_f}{b} + \ln\frac{h_{cap}}{h_f + h_{cap}}\right)\right]. \tag{35}$$

Clearly, as $h_{cap} \to \infty$,

$$\tau_{eff}^{DP} = S\,\frac{2G(1+\nu)}{(1-\nu)}\,\varepsilon - \frac{Gb(1-\nu\cos^2\alpha)\cos\phi}{2\pi h_f(1-\nu)} \ln\frac{\beta h_f}{b}\,, \tag{36}$$

where the contribution to the slowing-down of dislocation propagation [the right-hand side of Eqn (14)] is twice as large as the respective term in Eqn (15), which supports the above logical arguments.

Let us now turn to a heterostructure consisting of a buried strained layer whose thickness is much larger than the critical one. Such a heterostructure can actually be grown at low temperatures. Covered by a capping layer, the heterostructure is in a metastable state. If it is annealed at temperatures higher

than the growth temperature, the heterostructure undergoes plastic relaxation. When the relaxation process follows mechanism A, an increase in the thickness of the capping layer leads to a decrease in the average value of the elastic strain $\bar{\varepsilon}$, which would seem to lead to a decrease in the driving force of plastic relaxation of such a heterostructure. On the other hand, as noted earlier, a heterostructure in a metastable state must relax independently of the size of the capping layer. Figure 15 depicts the curves representing the dependence of the effective shear stress τ_{eff} on the thickness of the capping layer for the heterostructure $Ge_{0.3}Si_{0.7}/Si(001)$ 100 and 10 nm thick calculated by Eqns (32) and (35). The thickness of 100 nm exceeds the critical one by a factor greater than ten. Depositing a capping layer on such a structure should not significantly change the structure's metastable state. However, we see that the driving force of relaxation that proceeds according to mechanism A (a single misfit dislocation at the interface with the substrate) continuously decreases, which contradicts the reasonable assumption about the predetermined nature of the relaxation of such a heterostructure. Figure 15 shows that the possibility of injecting misfit dislocations via mechanism B in the form of dipoles remains significant and is almost independent of the capping layer thickness (curve *2* for a 100-nm thick layer). It is also clear that, starting from a relatively small thickness of capping layer, the relaxation of dipoles becomes more advantageous. The layer thickness of 10 nm is only slightly greater than the critical thickness ($h_c \sim 8$ nm; see Fig. 3). In this case, as Fig. 15 shows, calculations show a sharp decrease in the driving force of MD injection with increasing h_{cap} for both mechanisms, and the effective shear stresses, $\tau_{\text{eff}}^{\text{SM}}$ and $\tau_{\text{eff}}^{\text{DP}}$, vanish within the same range of capping layer thicknesses.

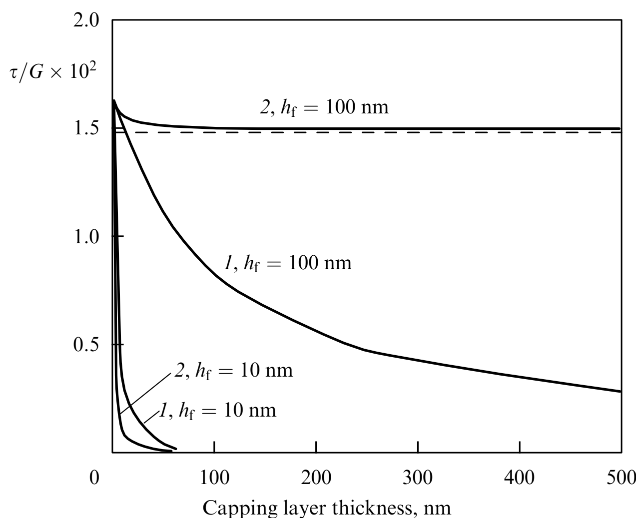

Figure 15. Dimensionless effective shear stress acting on (*1*) a single misfit dislocation and (*2*) on a dislocation pair as a function of the thickness of a capping layer for $Ge_{0.3}Si_{0.7}/Si(001)$ layers 100 and 10 nm thick (the results of calculations). \

3. Elastic relaxation

3.1 'Compliant' and 'soft' substrates

The physical mechanism that lies at the basis of the epitaxial transition from one material to another material with a different lattice parameter, used in conventional methods, is the relaxation of elastic strains in a thin layer of the new material via MD injection. However, MD injection irrevocably leads to generation of TDs that penetrate the epitaxially grown material, since a TD forms a common loop with misfit dislocations. The various conventional methods, which employ buffer layers with a varying lattice parameter, mesa structures on the substrate, or buffer layers consisting of strained-layer superlattices, are based on different ways of 'fighting' threading dislocations by facilitating the gliding of these dislocations toward the edges of the substrate (layer) or a mesa structure. In the last few years, new methods for growing artificial substrates have been developed. There are two groups of such substrates: 'compliant,' and 'soft.' The present section is devoted to the analysis of these methods.

When compliant and soft substrates are used, a completely different physical mechanism is assumed to operate, namely, the stresses are redistributed between the pseudomorphic layer and the thin (or soft) membranous substrate, as a result of which the pseudomorphic layer elastically relaxes without the formation of a misfit dislocation and, respectively, without the formation of a threading dislocation. Soft substrates, i.e., a layer of porous silicon (PS) or low-temperature silicon (LS) on the main silicon substrate, are characterized by an elevated concentration of point defects and smaller values of elastic constants and, supposedly, can be used as compliant substrates (a silicon membrane atop porous silicon) and as regions of preferable nucleation and multiplication of misfit dislocations.

3.1.1 Concept. The idea of using a compliant substrate is based on the effect related to the redistribution of elastic strains between the pseudomorphic layer and the substrate when the thickness of the latter is comparable to that of the growing layer (e.g. see Tkhorik and Khazan's monograph [68]). Figure 16 depicts the model of a device in which this effect can be realized. It is assumed that a thin membrane acting as a compliant substrate may freely move in the lateral direction without, however, disconnecting itself from the supporting thick substrate. Allowing for the substrate thickness, we can express the strains in the pseudomorphic layer by following formula [68]:

$$\varepsilon_f = \frac{d_0}{d_0 + h}\,\varepsilon_m\,, \qquad (37)$$

where d_0 and h are the thicknesses of the compliant substrate and the layer, respectively; ε_m is the total elastic strain, usually associated with the mismatch f of the lattice parameters of layer and substrate; and ε_f is the elastic strain in the layer. In

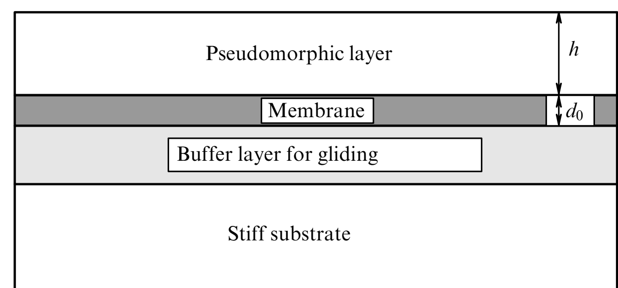

Figure 16. Schematic of a heterostructure that incorporates a thin membrane capable of sliding along the reference substrate.

this case, the elastic strain energy of the pseudomorphic layer becomes a nonlinear function of the growing-layer thickness:

$$E_{\mathrm{f}} = \frac{2G(1+\nu)}{1-\nu}\left(\frac{d_0}{d_0+h}\right)^2 f^2 h\,. \tag{38}$$

Plugging (37) into (14) instead of ε and making τ_{eff} equal to zero, we arrive at the equation

$$h_{\mathrm{c}}\,\frac{d_0}{d_0+h_{\mathrm{c}}}\,\frac{8\pi f(1+\nu)\cos\lambda}{b(1-\nu\cos^2\alpha)} = \ln\frac{\beta h_{\mathrm{c}}}{b} + 1\,. \tag{39}$$

If $d_0 \to \infty$ (thick substrate), Eqn (39) becomes (15). Figure 17 depicts an example of the graphic solution of Eqn (39) for $Ge_{0.3}Si_{0.7}$/Si(100). The solid curves represent the right-hand side of Eqn (39) as a function of h. The left-hand side of Eqn (39) is represented by dotted lines for different values of the membrane thickness d_0. The dotted curves intersect the solid curve at points corresponding to the critical thickness (in this case the right-hand side of Eqn (39) is equal to the left-hand side). If the membrane is thick ($d_0 \to \infty$, which is equivalent to a thick substrate), the intersection of the curve is at a point corresponding to h_{c} according to Matthews (the arrow in Fig. 17a). If the membrane is thin, the intersection point shifts to the right (as Fig. 17a clearly shows), i.e., the critical thickness increases. Finally, a moment comes when these curves cease to intersect (in Fig. 17a these are the left-hand sides of Eqn (39) at $d_0 = 5$ nm and 10 nm, with the corresponding curves being below the solid curve). In this case, the growing pseudomorphic layer has time to transfer the greater fraction of elastic strains to the membrane before MD injection becomes possible. The dependence of h_{c} on the membrane thickness is shown in greater detail in Fig. 18. Clearly, at small values of d_0 the critical thickness tends to infinity. We also see that the redistribution of the stresses between the pseudomorphic layer and the thin substrate, which has a significant effect on h_{c}, manifests itself only for small membrane thicknesses. In the case at hand, at $x = 0.3$, this effect becomes significant for membranes thinner than 30 nm. Figure 19 depicts curves representing the dependence of the critical thicknesses on the mismatch between the lattice parameters of layer and substrate calculated for various membrane thicknesses by Freund and Nix [69] (a) and Zhang and Su [70] (b). For the sake of comparing of these two calculations, the dashed straight lines represent the sections corresponding to the strains in a pseudomorphic $Ge_{0.3}Si_{0.7}$/Si(001) layer.

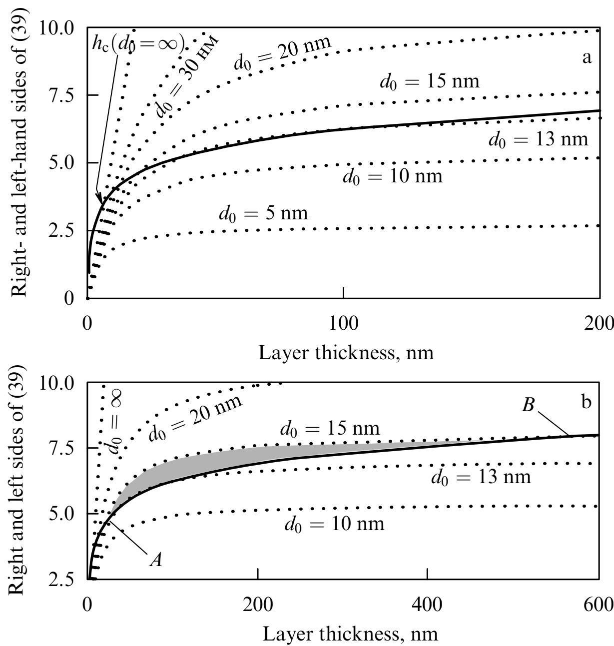

Figure 17. Example of the graphic solution of Eqn (39) for $Ge_{0.3}Si_{0.7}$/Si(100). The solid and dotted curves represent the right- and left-hand sides of Eqn (39) (see explanations in the main text).

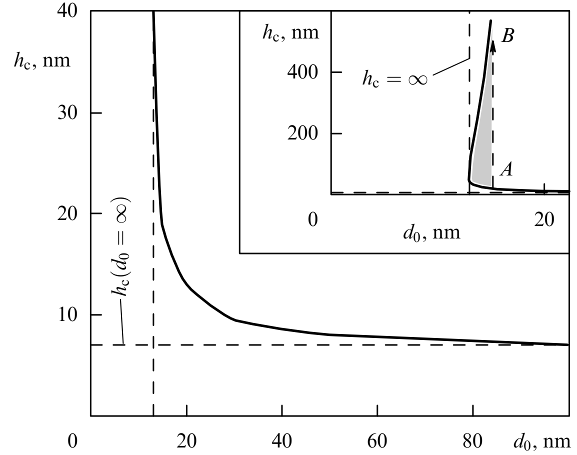

Figure 18. Increasing critical thickness of the Ge_xSi_{1-x}/Si(100) layer with decreasing membrane thickness d_0 at $x = 0.3$. The inset shows the same diagram on a different scale. The curves represent the results of calculations.

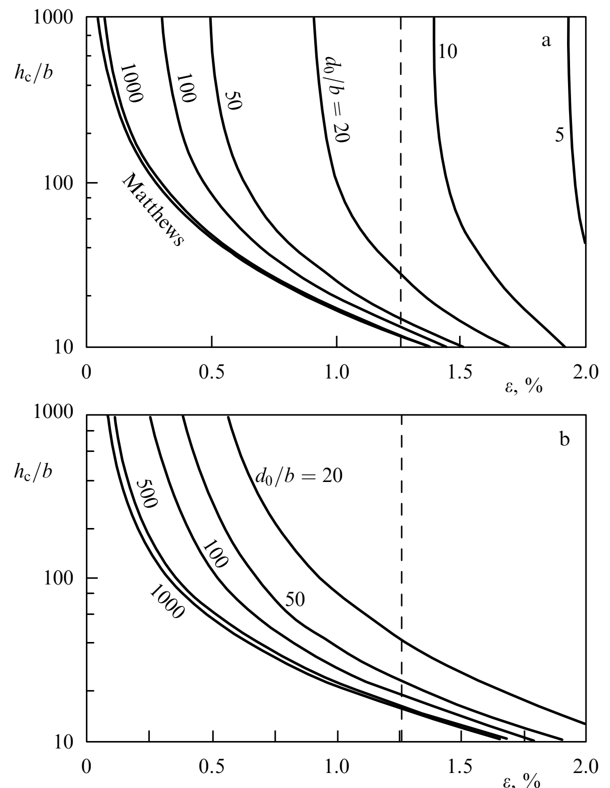

Figure 19. Dependence of normalized critical thickness for MD injection on strains in the heterostructures and the membrane thickness d_0 (in nanometers). The results have been taken from Refs. [69] (a) and [70] (b).

A graphic solution, an example of which is depicted in Fig. 17, makes it possible to also qualitatively analyze the transition of a strained layer from plastic relaxation to elastic relaxation and to discover features that so far have not been discussed in the literature. Figure 17a clearly shows that the curves representing the left- and right-hand sides of Eqn (39) in the region of the transition to $h_c \to \infty$ intersect at an acute angle (e.g., see the curve for $d_0 = 13$ nm). The logarithmic part of (39) is not known too well; e.g., Houghton [20] assumes that $\beta = 4$, while Gillard et al. [4] put this value at 0.76. Accordingly, such a spread in the value of β creates a substantial indeterminancy in the theoretical calculation of the membrane thickness at which $h_c \to \infty$.

We believe, however, that the case where a pseudomorphic layer is in a metastable state within a limited interval of thicknesses is more important (so far this state has not been mentioned in the publications in this area of research). The effect is clearly seen in Fig. 17b, in which the curves have been continued into the region of large thicknesses of the growing layer. Despite the fact that the curve for $d_0 = 15$ nm intersects the solid curve at point A, farther from this point, as the layer thickness increases, the dashed curve passes above the logarithmic curve, and then intersects it in the opposite direction (point B in Fig. 17b). Thus, there is a certain region (hatched region in Fig. 17b) in which the pseudomorphic layer can be in a metastable state only within a limited interval of thicknesses. Here, the driving force for MD injection, the effective shear stress τ_{eff}, is substantially lower. For instance, for a 20-nm thick membrane the driving force for MD injection decreases by a factor of approximately 17 for a layer that is 100 nm thick and by a factor of approximately 34 for a layer that is 200 nm thick in comparison to the case without a membrane. In view of existing kinetic limitations on MD injection, such a layer, despite the fact that it temporarily finds itself in the metastable region, remains in the elastic state, which broadens the possibilities of using compliant membranes of various thicknesses and makes it less crucial if we know the exact value of d_0 at which h_c becomes infinite. The dashed area in the inset in Fig. 18 corresponds to the dashed area in Fig. 17b. Thus, in pseudomorphic layers grown on thin membranes the driving force for plastic relaxation, the effective shear stress τ_{eff}, decreases markedly.

3.1.2 Fabrication of compliant substrates. The first to point to the possibility of using a thin substrate as an object lifting the stresses in a growing layer before it reaches critical thickness was Y H Lo. In his experiments (see Ref. [71]), Lo showed that this is indeed possible using thin membranes, which were fabricated by etching holes in the substrate of a specially grown heterostructure. In the process of growing a strained layer, such membranes became bent, with the result that the experiments were purely demonstrative in nature. At present, there are two promising variants of fabricating compliant substrates.

GeSi/SOI. The use of 'silicon-on-insulator (SiO_2)' substrates. The substrate consists of a thin layer of silicon 10–100 nm thick bonded to an oxide interlayer (SiO_2). The latter in turn is placed atop of a thick substrate [72, 73]. In a variant of this method used for III–V compounds, the heterostructure GaAs/AlGaAs/GaAs is bonded to the reference substrate with an intermediate layer acting as a 'soft' substrate in between. Then different etchants are applied to the substrate of the heterostructure GaAs and the AlGaAs layer (AlGaAs is used as a blocking layer in etching the GaAs substrate just as in the well-known technique of photocathode fabrication (e.g., see Refs. [74, 75])). The remaining GaAs layer on the 'soft' sublayer becomes the compliant substrate in growing strained InGaAs layers [76].

Bonding with a twist. In this case, the heterostructure (e.g., GaAs/AlGaAs/GaAs) is bonded directly to the GaAs substrate without an intermediate layer being present, with the crystallographic orientations of the bonded pair not coinciding in angle, i.e., a twist around an axis perpendicular to the surface is enforced. At the interface, a network of purely screw dislocations forms, whose density increases with the angle of twist. Then, the GaAs substrate and the blocking layer of the AlGaAs heterostructure are etched in the same way as in the previous method. It is assumed that, as a result of further growth of the strained layer (e.g. InGaAs on a thin GaAs layer), this layer becomes compliant, since the region with the screw dislocations facilitates the sliding of the layer along the reference substrate [77].

The theory of the two methods has also been developed (e.g., see Refs [69, 70, 78, 79]).

3.1.3 Commentary. The literature on these two methods contain experimental data that corroborate the validity of the concept discussed in Section 3.1.1. However, there still is a purely technological contradiction: the intermediate 'soft' layer must be compliant in the substrate plane but 'stiff' in the growth direction. Another contradiction also seems to be unresolvable, i.e., if the growing layer first grows as a pseudomorphic layer and then relaxes without misfit dislocations (according to the concept discussed in Section 3.1.1, the stresses in this layer are transferred to the compliant layer, with the result that strains develop in the latter), it must slide along the substrate over large (on the atomic scale) distances, which is impossible without spalling. Probably for this reason the literature on the subject does not contain data (or at least commentaries) on growing perfect layers on large-area compliant substrates.

It also seems to be highly unlikely that in the case of a substrate with a network of screw dislocations the relaxation of a growing strained layer is purely elastic: an interlayer with a high density of imperfections is an effective source of misfit dislocations, which penetrate the initial pseudomorphic layer.

The possible improvement of the structural properties of a pseudomorphic layer due to the 'softness' of the substrate has so far been estimated only theoretically. Jesser and Fox [47], in calculating the effect of the properties of a compliant substrate on the critical thickness of a pseudomorphic layer, emphasize the importance of reducing the values of the elastic constants of the substrate, but the main emphasis is on reducing the substrate thickness.

3.1.4 Porous silicon as a substrate. As noted earlier, the idea of a compliant substrate is based on fabricating a membrane, a thin substrate, that would take upon itself the strains in the growing layer. Here, the elastic constants of layer and substrate are assumed equal [Eqn (37)]. In the general case, the thin substrate may be characterized by different values of the elastic constants. Then, the mechanical equilibrium of the layer–substrate system can be written as follows:

$$G_{\text{f}} \frac{1+\nu_{\text{f}}}{1-\nu_{\text{f}}} \varepsilon_{\text{f}} h + G_0 \frac{1+\nu_0}{1-\nu_0} \varepsilon_0 d_0 = 0 \,, \tag{40}$$

where the zero in the subscript refers to the thin substrate. Ignoring the difference in the Poisson ratios and allowing for the fact that $\varepsilon_f - \varepsilon_0 = \varepsilon_m$, we obtain

$$\varepsilon_f = \frac{1}{1 + G_f h / G_0 d_0} \, \varepsilon_m \, . \tag{41}$$

Clearly, a decrease in the value of the shear modulus G_0 in the thin substrate has the same effect as a decrease in the thickness of that substrate. To make this reasoning more graphic, in Fig. 20a we depict two dependences characterizing the decrease in elastic strains in the layer with the increase in the layer-to-membrane thickness ratio h/d_0. A decrease in the shear modulus characterizing the membrane by a factor of ten significantly reduces the size of the elastic strains in the strained layer. Accordingly, the elastic strain energy of the layer is a complicated function of the layer thickness:

$$E_f = Y \varepsilon_f^2 h = \frac{Y f^2 h}{(1 + G_f h / G_0 d_0)^2} \, . \tag{42}$$

Figure 20b depicts the energy of the pseudomorphic layer normalized to Young's modulus Y and the square of the mismatch energy f in dimensionless form,

$$\frac{E_f}{Y f^2 d_0} = \frac{h/d_0}{(1 + G_f h / G_0 d_0)^2} \, , \tag{43}$$

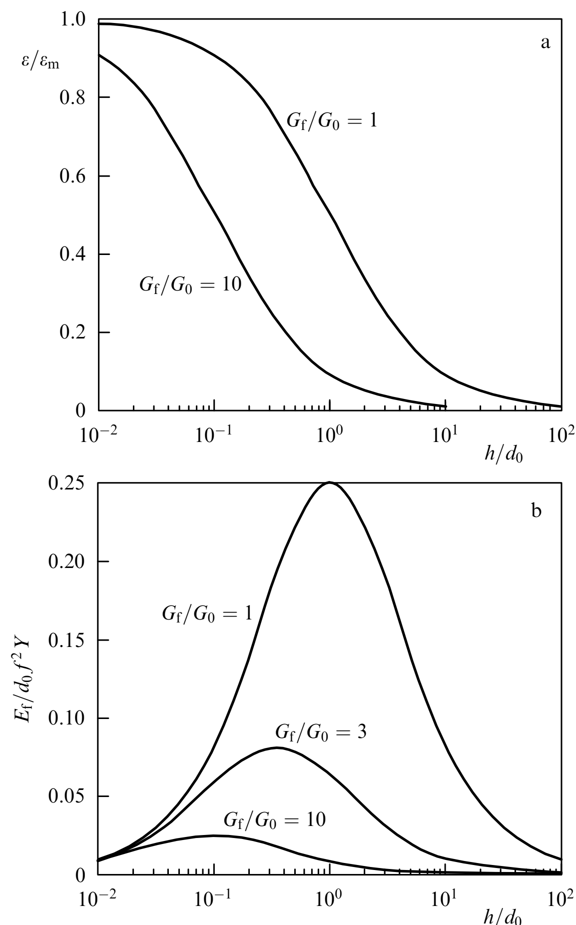

Figure 20. (a) Elastic strains in a pseudomorphic layer and (b) the energy of the layer as functions of the film-to-membrane thickness ratio for several values of the shear modulus ratio (the results of calculations).

as a function of the layer-to-membrane thickness ratio h/d_0 for three ratios G_f/G_0 equal to 1, 3, and 10. A decrease in the shear modulus of the membrane leads to a significant drop in the maximum possible value of the stress energy stored in the layer, while the peaks in the curves shift to the right, i.e., in the direction of relatively large membrane thicknesses.

In the commonly used semiconducting materials, the ratio of elastic constants varies in the vicinity of 2, while the membrane thickness can be varied within broad limits. Accordingly, in developing the concept of a compliant substrate, attention has been focused on the fabrication of thin membranes. However, the last few years have seen the emergence of a new material, porous silicon, whose elastic constants may differ substantially from those of bulk silicon. For instance, according to Bellet [80], Young's modulus decreases by several dozen times at porosities reaching 90%. Hence, attention should be focused on the shear modulus G_0 in (41), whose small value leads us to the soft-substrate model (i.e., to a substrate that, due to its softness, takes on the main part of the strains of the growing strained layer), while the special features of the curves shown in Figs 20a and 20b can be exploited in some manner. In a recent investigation by Romanov et al. [81], porous silicon was used as a substrate that was both soft and compliant. The researchers showed that layers of the $Ge_{0.3}Si_{0.7}$ solid solution remain plastic and unrelaxed for thicknesses up to 0.3 μm.

3.2 Elastic relaxation of layers via island formation

As noted in Section 2.4, the surface of a strained layer may become rough during growth of the layer or annealing in accordance with the elastic relaxation mechanism. This effect has been actively studied in the last ten years in connection with its key significance in the formation of a special state of the strained layer in the form of nanometer-sized islands. The main idea of the model is that, thermodynamically, the rough surface of a strained layer (and the more so the island structure of the surface) is more at equilibrium due to the elastic stress relaxation at the tips of the islands. The surface energy of the layer is the counteracting factor, but it is only partially balanced by the tendency of the system to move into a state with a rough surface. The mechanism by which this phenomenon is realized is the movement of the growth units along the surface to places with the lowest free energy, i.e., to the apexes of the rippled surface. Knowing the special features of elastic relaxation in detail is necessary in order to combat the roughness of strained layers and to achieve the opposite goal, i.e., to fabricate nanoislands with a high density. Hence, the given model was rapidly recognized by the scientific community, with the result that from 1990 – 1995 many theoretical and experimental papers aimed at substantiating it appeared.

3.1.1 Historical discourse. Below we give a chronological list of the main papers from which the main ideas of the model can easily be extracted.

1972. Asaro and Tiller [82] theoretically examine the problem (for an abstract physical object) of the effect of stresses on the morphological stability of a surface and found that the instability of the surface, being required by the laws of thermodynamics, may develop due to surface diffusion of atoms.

1986. Grinfel'd [83] theoretically shows that the surface of a nonhydrostatically stressed solid in contact with its liquid phase is unstable against perturbations of any wavelength if

the particles of the substance are able to migrate along the surface. The instability appears under nonhydrostatic stresses no matter how small these stresses are. Surface tension suppresses this instability in the short-wavelength part of the spectrum.

1988. Berger et al. [84] are the first to state irrevocably that the free energy of a strained layer reaches its minimum at a certain value of the surface roughness. Experiments show that the surface lattice parameter of the $In_{0.35}Ga_{0.65}As$ layer on GaAs increases with the layer thickness until this thickness remains smaller than the critical one, i.e., the surface sections of the growing layer undergo elastic relaxation. In 1989, Srolovitz [85] is the first to develop a theory of instability of the flat surface of a strained solid that holds for pseudomorphic semiconducting InGaAs layers on GaAs, the theory being based on the experimental results of Berger et al. [84].

1990. Eaglesham and Cerullo [86] show by their experiments that germanium islands on Si(100) are free of misfit dislocations up to thicknesses that exceed the critical thickness by a factor of 50. An explanation of this phenomenon is based on the assumption that an island and the surrounding area of the substrate undergo elastic relaxation. In the same year, Guha et al. [87] obtained direct experimental proof that islands of $In_{0.5}Ga_{0.5}As$ on GaAs whose thickness substantially exceeds the critical one undergo elastic relaxation. The investigations were carried out using a high-resolution transmission electron microscope to study a transverse section. (Note that this was the first time that nanometer-sized islands were studied in this way.) The lattice parameter of the apex of a dislocation-free island becomes equal to that of the unstrained $In_{0.5}Ga_{0.5}As$ solid solution. After these publications appeared, there was a sharp increase in the number of papers dealing with the mechanisms of strained island formation and the ordering of such islands, since the possibility appeared of fabricating arrays of defect-free (i.e., containing no misfit dislocations) 3D objects of nanometer dimensions, which found practical applications in nanoelectronics. In the same year, Mo et al. [88] use scanning tunneling microscopy (STM) to demonstrate the existence of well-defined 3D islands of Ge on Si and determine their faces to be {105}. The researchers called these islands hut-clusters.

1991. Snyder et al. [89] use reflection high energy electron diffraction (RHEED) and STM to study the evolution of surface morphology of InGaAs on GaAs(100) and establish that there is a relationship between the morphology of the layer surface and strain relaxation in the layer. They propose a new mechanism of relaxation of strained layers: elastic relaxation via coherent islands.

1992. Cullis et al. [90] show that there is a relationship between the roughness of the surface of the GeSi solid solution and the variations of the strains in the layer. This fact is explained by the presence of partial elastic relaxation of the strains in the surface asperities. The silicon layer that caps this surface smooths the layer out.

The above publications became the starting point for the various theoretical studies devoted to the instability of the surface of a growing strained layer for specific heterostructures: GeSi on Si, and InGaAs on GaAs. Among these are the studies of Ratsch and Zangwill (1993) [91], Spencer et al. (1993) [92], Freund and Jonsdottir (1993) [93], Tersoff and LeGoues (1994) [39], Johnson and Freund (1997) [94], Obayashi and Shintani (1998) [95], and Müller and Kern (1998) [96].

3.2.2 Results of theoretical calculations. Figures 21 and 22 depict the results of the theoretical calculations belonging to the two approaches to the mathematical model of elastic relaxation of strained layers: the integral approach, i.e., for the entire surface of the layer in connection with the GeSi/Si system [95], and the approach in which the calculation is done for a separate island. What lies at the basis of both approaches is the calculation of the equilibrium state of the rough surface of the strained layer, which amounts to minimizing the sum of the stress energy and the surface energy. This complicated problem is solved under the assumption that both the elastic and surface properties of the system are isotropic. Neither is the nonmonotonic nature of the surface properties of the layer during the emergence of vicinal faces taken into account. (Kern and Müller [97] and Pehlke et al. [98] performed calculations that took into account the surface energy of specific faces and the more subtle effects related to the influence of stresses on the surface energy.)

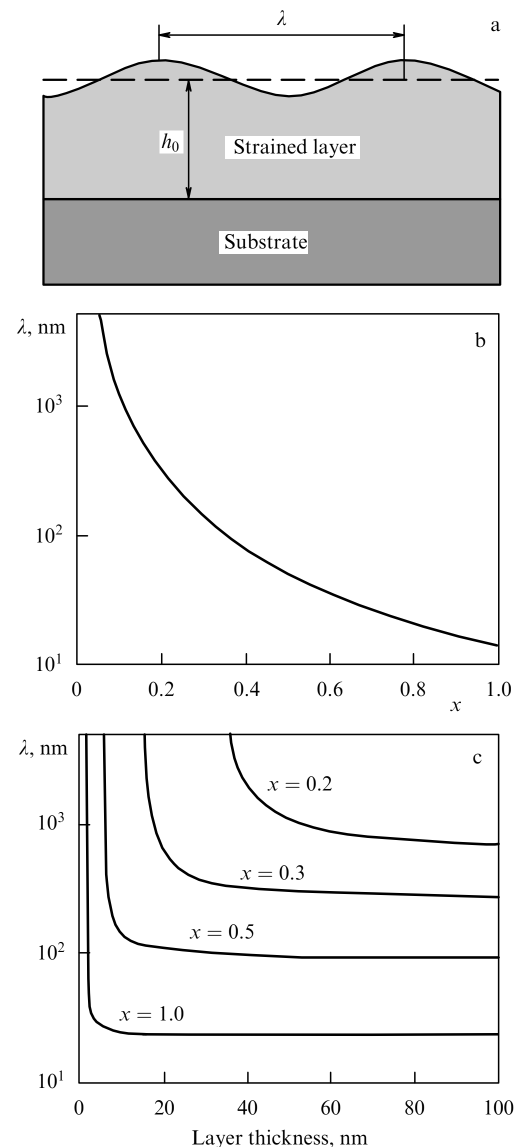

Figure 21. The Obayashi and Shintani model [95]: (a) the geometry of the model, and curves representing the dependence of the critical wavelength λ of the roughness of the strained heterostructure $Ge_xSi_{1-x}/Si(100)$ on (b) the composition x and (c) the layer thickness.

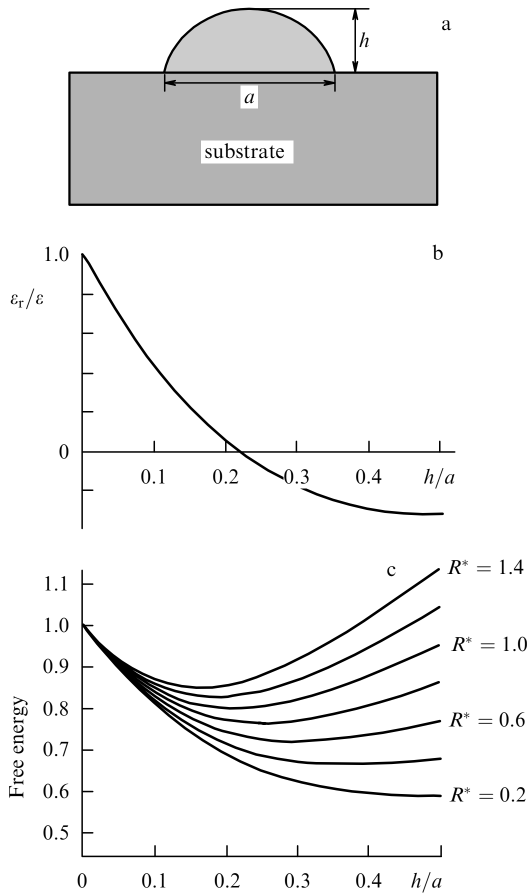

Figure 22. The Johnson and Freund model [94]: (a) the geometry of the model, and the variations of (b) the elastic strain at an island apex and (c) of the island's total free energy normalized to unit volume as functions of the geometric parameter of the island h/a.

Figure 21 depicts a model in which a surface wave diminishing the stresses is introduced for a strained GeSi/Si layer of certain composition and thickness. At a certain wavelength (known as critical), a quasi-equilibrium state is set in in the system. Figure 21b shows that the critical wavelength decreases with increasing germanium concentration in the solid solution and amounts to about 20 nm at $x = 1$, which is in good agreement with the dimensions of the islands discovered in this system by TEM and STM (e.g., see Ref. [99]). Figure 21c depicts the critical wavelength as a function of the thickness of the pseudomorphic layer for different compositions. Clearly, at a certain layer thickness, which increases with decreasing germanium concentration in the layer, the critical wavelength reaches a plateau. Another conclusion that can be drawn from this figure is that the surface of the strained layer is unstable even for small germanium concentrations in the layer ($x = 0.2$ in Fig. 21c), which corroborates the theoretical conclusion drawn by Grinfel'd [83] discussed in Section 3.2.1. The conclusion is also corroborated by modern experimental data (see the papers by Floro et al. [100] and Ozkan et al. [101]); the surface of the layer is unstable even for small mismatches with the substrate, the only requirement being that the temperature rise so that surface diffusion is expedited.

Figure 22 depicts a model used to calculate the minimum of the free energy for a coherent island in the form of a hemisphere. The main parameter here is the ratio of the height of the island to the island's lateral size, h/a (the aspect ratio), on which the degree of elastic relaxation of a coherent island strongly depends. Figure 22b clearly shows that the size of the elastic strains at the island apex depends on the island's dimensions, decreasing with increasing h/a. Figure 22c demonstrates the change that the total free energy of an island undergoes as h/a increases. Here, the minimum shifts to the right along the h/a axis as the parameter R^* decreases. This parameter is introduced as the measure of the ratio of the surface energy γ to the energy of elastic strains (proportional to ε^2):

$$R^* = \frac{2\gamma}{M\varepsilon_{\mathrm{m}}^2 A^{1/2}}\,, \tag{44}$$

where $M = 2G(1+\nu)/(1-\nu)$, with G, ν, and γ being the shear modulus, the Poisson ratio, and the surface energy, respectively; A is the area of the island – substrate interface; and ε_{m} is the same quantity as in Eqn (37). The stress energy is in the denominator. Thus, the greater the elastic strains, the smaller the parameter, the deeper the minimum in the free energy, and the farther this minimum is along the h/a axis, corresponding to larger magnitudes of the roughness. Here, one can clearly see the role of the surface energy, which is in the denominator of Eqn (42) for the parameter R^*.

3.2.3 Experimental verification of the model. The emergence and development of morphological instability in the surface of a strained epilayer become more intense as the mismatch between the lattice parameters of layer and substrate becomes greater. A rise in temperature shifts the beginning of the emergence of a rough surface into the region of smaller initial strains. The roughness of the surface of a strained layer also increases with the layer thickness. The literature contains solid proof that these laws hold [100, 102 – 104].

If the surface energy of the new phase is lowered in some way, the layer may lose its morphological stability even when the mismatch is small. For instance, when there is contact between a strained layer and the liquid phase, in which case the surface energy of the layer is much lower than the surface energy of the layer – vacuum (or vapor) interface, islands form in the $Ge_xSi_{1-x}/Si(001)$ system at very small mismatches corresponding to a germanium concentration $x \sim 0.05$ ($\varepsilon \sim 0.2\%$) [105]. The dimensions of the islands and the roughness period are on the order of one micron, so that both islands and surface roughness can easily be observed. The surface waves of roughness and the islands align themselves along the $\langle 100 \rangle$ directions, while misfit dislocations are not observed [105].

In conclusion to this section, we formulate the following statements: (a) the driving force of morphological instability of a strained layer always exists for all layer thicknesses and increases with thickness and the difference in the lattice parameters of layer and substrate; and (b) to diminish the roughness, surface diffusion processes must be suppressed, to which end one should lower the growth temperature and also employ methods that facilitate planarization of the surface of the strained layer, e.g., use surface-active substances or capping layers.

3.2.4 Surface roughness and misfit dislocation injection. The irregularities that form on a surface lower the barrier for nucleation of dislocation half-loops, and, at a certain value of roughness, plastic relaxation of the epilayer via MD injection

from the surface becomes possible. The assumption that this is how the events develop provided a convenient explanation for the experimentally observed plastic relaxation of layers with initial strains lower than 1.5%, at which level it is highly unlikely for dislocation half-loops to form on a smooth surface (see Section 2.4). However, the situation proved to be not so simple. For instance, Dorsch et al. [105] found that no misfit dislocations formed in $Ge_xSi_{1-x}/Si(001)$ layers with $x \sim 0.5$ disintegrated into separate islands, despite the fact that the island thickness exceeds the critical one.

A similar roughness structure is observed during the annealing in vacuum of initially planar $Ge_xSi_{1-x}/Si(001)$ layers grown by MBE. Ozkan et al. [101] thoroughly studied the morphological changes of the surface of such epilayers by such mutually complementary methods as TEM, atomic force microscopy (AFM), and X-ray diffraction. The researchers discovered that surface roughness aligns itself along the $\langle 100 \rangle$ directions irrespective of the layer thickness, due to the special features of the anisotropy of the elastic properties of the crystal surface of the given material. [The same orientation of the surface formations was observed by Cullis et al. [106] in the InGaAs/GaAs(001) system.] Correspondingly, the walls of these structures do not coincide with the planes that are most suitable for the formation of dislocation loops. In epilayers whose thickness exceeds the critical one, the MD network that was formed (in the directions $\langle 110 \rangle$) reorganizes the orientation of the morphological surface waves from $\langle 100 \rangle$ to $\langle 110 \rangle$ (see Ref. [101]). Such rotation can be explained by the effect of the stress field of the MD network, which generates a lateral chemical potential gradient at the surface of the layer, which facilitates the transformation of the morphological structure of the surface via surface diffusion. As a result, the 'valleys' and 'ridges' assume a direction 'imposed' by the elastic strain field of the misfit dislocations.

Cullis et al. [106, 107] conducted similar investigations. They studied InGaAs/GaAs(001) heterostructures and found that under standard growth conditions the morphological instability of the surface of a strained epilayer, i.e., the transition from 2D to 3D growth, is observed in samples with $\varepsilon > 1.5\%$ (Peiro et al. [108] also found this to be true for InGaAs/InP(001)). It is assumed that the 'valleys' on the surface of a strained epilayer and their intersections are suitable places for the nucleation of dislocations, since in these places the stresses are higher. However, when these heterostructures were examined under an electron microscope, mainly short dislocation segments were discovered in heterostructures based on GeSi [101, 109] and InGaAs [106, 107]. Studies of the transverse sections of these heterostructures indeed revealed the presence of defects related to 'valleys,' but such defects have a complicated structure, which is discussed in the above-cited papers.

Thus, it has now been established that there is a certain relationship between the loss of morphological stability of strained epilayers and MD formation, but this relationship manifests itself clearly only in heterostructures with a medium ($\varepsilon \sim 1.5\%$) and higher strain level. On the other hand, these studies were unable to corroborate the assumption (popular earlier) that the roughness of a surface is the main source of misfit dislocations in heterostructures with small mismatches ($\varepsilon < 1.0\%$). The new possibilities of observing surfaces with atomic resolutions have shown that misfit dislocations appear in such heterostructures notwithstanding the 2D mechanism of growth [106].

4. Surface morphology of relaxed epilayers

As we have seen from the previous section, an MD network at the epilayer – substrate interface generates a stress field that reaches the layer surface and affects the growth mechanism. This results in the emergence of a characteristic structure of the surface in the form of intersecting bands (cross-hatch patterns) (see Ref. [110] and the papers cited therein). The protrusions and depressions of the surface relief are aligned along the $\langle 100 \rangle$ directions corresponding to the intersection of the inclined glide planes of 60° dislocations and the substrate plane (100) or (111). As early as 1975, Olsen [111] used TEM and optical microscopy to establish the relationship that exists between the emergence of characteristic bands on the surface of an epilayer (which were later called cross hatches) and the discovery of misfit dislocations at the layer – substrate interface. Twenty years later, Lutz et al. [112] showed that there is a direct relationship between the dislocations and the size of the surface steps. Single misfit dislocations produce a step on the surface of the GeSi/Si(001) layer whose calculated shape is depicted in Fig. 23a. Modern methods used in studying surface morphology (AFM in this case) make it possible to detect steps of this size. In Figure 23b, the calculated shape of a step generated by five misfit dislocations from a single source (in the inset) is compared with the appropriated AFM profile of a relaxed GeSi/Si(001) sample.

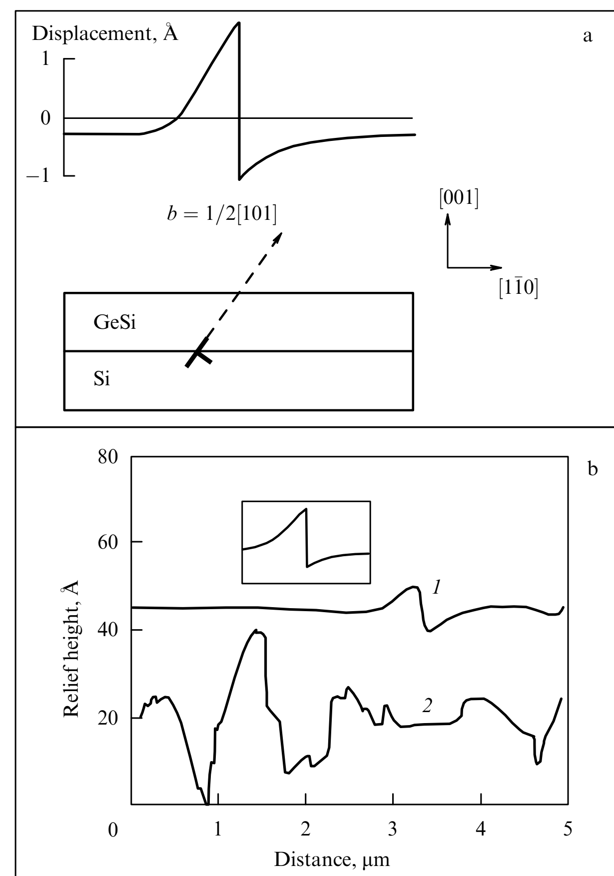

Figure 23. Steps on the surface of a strained layer caused by misfit dislocations. The figure shows the results of calculations when (a) there is only one misfit dislocation and when there is a cluster of five misfit dislocations (the inset in Fig. 23b); Curves *1* and *2* represent the results of measurements (all results have been taken from Ref. [112]).

Clearly, the agreement between the calculated and experimentally determined step shapes is satisfactory.

As the epilayer becomes thicker and especially at high growth temperature, a new mechanism begins to strongly affect the morphology of the growing surface. According to this mechanism, proposed by Fitzgerald and others (e.g., see Ref. [113]), the stress field from the dislocation network facilitates the transformation of the surface (see the previous section). Superimposing several growth mechanisms for layer surface roughness makes the surface profile more complicated and increases the amplitude of undulations of the relaxing-layer thickness. As a result, we get a surface with a coarse relief (e.g., the relief shown in Fig. 23b, curve *2*).

Thus, the main reasons for the formation of a cross-hatch pattern on the surface of a relaxing strained layer are the loss of morphological stability of the layer due to the elastic relaxation of the strained layer, the presence of steps due to the injection of separate dislocations and dislocation packets, and the effect of the stress field of an MD network on the rate of growth of separate sections of the surface. The resulting picture of the surface morphology of the layer is the superposition of these three mechanisms of roughness growth. Depending on the conditions of growth (temperature, the amount of misfit, and layer thickness), each of these three mechanisms may become decisive.

5. Practical realization of the relaxation mechanisms

5.1 The main physical prerequisites for using GeSi/Si heterostructures in devices

By the end of 2001, the world market for electronic appliances is expected to reach a value of US $ 200,000,000,000. It is also well known that 97% of that market is based on silicon electronics. The most rapidly developing segment of the market is communication devices and equipment, and it is in this segment that high-quality and, at the same time, cost-effective digital components and small integrated circuits of the microwave band are required. It is here that Ge_xSi_{1-x}/Si heteroepitaxial structures have found their widest application, even somewhat undermining the fairly recent monopoly of III – V semiconducting compounds. Note that in their limiting characteristics devices based on GeSi/Si heterostructures will always be inferior to those based on AlGaAs/GaAs heterostructures. However, for a broad range of electronic appliances the limiting characteristics are never reached, and what is decisive here is the cost-effectiveness and the compatibility with other elements of electronic circuits, and with respect to these parameters GeSi/Si heterostructures have proved to be quite competitive.

For any heterostructure, the possibility of using it in a microwave transistor is determined primarily by the mobility and concentration of the 2D electron (or hole) gas that is formed in the heterojunction by the modulation doping method. To achieve high mobility, the heterojunction must be atomically smooth and contain no dislocations, and there must also be a minimum number of background (uncontrollable) impurities. More than that, the very formation of the 2D electron or hole gas is possible only if there are band discontinuities of necessary magnitude and sign in the heterojunction. In contrast to the AlGaAs/GaAs heterostructure, in which the mismatch in the lattice parameters is negligible, in GeSi/Si the elastic strains play a decisive role in forming the electronic properties of the heterojunction and serve as one of the main instruments of band engineering. We will now briefly discuss these effects.

Silicon and germanium are indirect-gap semiconductors with band gaps at room temperature equal to 1.124 and 0.665 eV, respectively [114]. Silicon has six valleys in the conduction band near point X of the Brillouin zone, which are characterized by two components of the effective-mass tensor, the longitudinal component $m_l/m_0 = 0.916$ and the transverse component $m_t/m_0 = 0.19$. Here, the effective conduction-electron mass amounts to $m_c/m_0 = 0.259$. The absolute minimum of the conduction band of germanium is at point L of the Brillouin zone, and the four valleys are characterized by the following components of the effective-mass tensor: $m_l/m_0 = 1.57$ and $m_t/m_0 = 0.087$ (the effective conduction-electron mass of germanium is $m_c/m_0 = 0.118$). In accordance with such a band structure, the electron mobilities for the undoped silicon and germanium crystals at 300 K amount to 1450 and 3900 $cm^2\ V^{-1}\ s^{-1}$, respectively. The constant-energy surfaces of the two upper valence bands in Si and Ge, which are degenerate at point Γ of the Brillouin zone, are anisotropic and nonparabolic. In many cases these complications are ignored and the values of the effective masses of the light and heavy holes are taken in the spherical approximation ($m_{lh}/m_0 = 0.159$ and $m_{hh}/m_0 = 0.467$ for Si, and $m_{lh}/m_0 = 0.0424$ and $m_{hh}/m_0 = 0.316$ for Ge). The hole mobilities for undoped silicon and germanium at 300 K are 450 and 1900 $cm^2\ V^{-1}\ s^{-1}$, respectively.

The redistribution of the charge of the valence electrons at the heterojunction leads to the formation of a dipole layer, and the elastic strains shift and split the corresponding energy levels. Liu et al. [115] did the necessary calculations, whose results for a pseudomorphic germanium layer on an Si(100) substrate are depicted in Fig. 24b and for a pseudomorphic silicon layer on Ge(100), in Fig. 24c. Clearly, the arrangement of the bands facilitates the formation of a 2D hole gas in pseudomorphic germanium layers (or a Ge_xSi_{1-x} solid solution) grown on a silicon substrate and a 2D electron gas in pseudomorphic silicon layers grown on a germanium substrate (or Ge_xSi_{1-x}). It is also clear that gigantic non-hydrostatic strains lead to gigantic changes in the band structure. For instance, the band gap of a pseudomorphic silicon layer on a germanium substrate is twice as small as that of an unstrained bulk crystal. What we have just said is not the only effect of strain on the electron properties of Si/Ge heterojunctions. In addition to lifting the degeneracy of the valence bands at point Γ, biaxial compression of a pseudomorphic germanium (or Ge_xSi_{1-x}) layer on a silicon substrate also substantially changes the dispersion law $E(\mathbf{k})$. For one thing, the effective mass of the 'heavy' holes in the valence band $E_{v2}^{Ge}(hh)$ (Fig. 24b) proves to be smaller than the effective mass of the 'light' holes in the valence band $E_{v1}^{Ge}(lh)$. In other words, the holes that were 'heavy' in unstrained bulk germanium become 'lighter' than the 'light' holes in the pseudomorphic layer. Since at room temperature and in a wide range of charge-carrier concentrations the mobility is inversely proportional to the square of the effective mass, the gain in mobility (with all other things being equal) reaches a value of the same order as that in pseudomorphic $Si_{0.5}Ge_{0.5}$ layers [116].

Elastic tensile strain in a pseudomorphic silicon layer on relaxed buffer Ge_xSi_{1-x} layers facilitates an increase in electron mobility due to the splitting of the sixfold-degenerate conduction band into two constant-energy ellipsoids

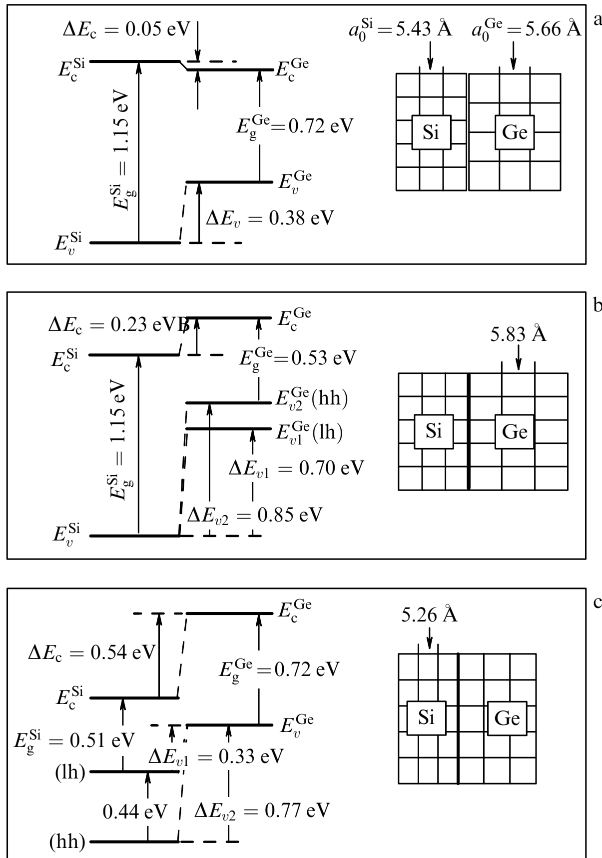

Figure 24. Band diagrams of the Ge/Si heterojunction: (a) without allowance for elastic strains and dipole effects; (b) for a pseudomorphic Ge layer on a Si(001) substrate, and (c) for a pseudomorphic Si layer on a Si(001) substrate.

with the major axes directed perpendicular to the current and four ellipsoids lying in the plane of the 2D electron gas. Such reconfiguration of the band structure leads to a substantial decrease in the intervalley scattering on f-phonons, which changes the electron quasi-momentum by 90°, but does not affect the much weaker intervalley scattering on g-phonons, which changes the electron quasi-momentum by 180°. The combination of all these factors 'guarantees' that the electron mobility in a channel can be as high as 2900 cm^2 V^{-1} s^{-1} and the hole mobility, as high as 1800 cm^2 V^{-1} s^{-1} [117], which in turn has made it possible to fabricate field-effect transistors capable of operating at 70 – 80 GHz.

The advantages of GeSi/Si heterojunctions over common silicon are so great that the leading manufacturers of integrated circuits have already announced the use of pseudomorphic Si/GeSi/Si heterostructures in their production lines for manufacturing chips for microwave electronics and memory circuits with the use of CMOS technology [118].

5.2 Artificial substrates

To fabricate various semiconductor devices that use the entire spectrum of semiconducting materials whose epitaxial growth technology has been thoroughly developed, it is advisable to have a set of substrates that are based on Si and GaAs and ensure growing heterostructures with different lattice parameters. Such substrates are usually said to be artificial. Thus, by an artificial substrate we mean a heterostructure that is grown epitaxially on a commercially available silicon (or GaAs) substrate and has a new market quality: a perfect crystal structure and smoothness of surface differing little from the base substrate, but a different lattice parameter. This makes it possible to fabricate device heterostructures based on solid-solution layers (or III – V compounds) with improved characteristics.

Simply growing GeSi layers on silicon substrates did not lead to success, since the number of threading dislocations in such layers rapidly increases with the germanium concentration. According to the literature on the subject (see Refs [1, 16, 37]), the characteristic TD density in layers of constant composition and its dependence on x follows the curve depicted in Fig. 25. The high TD density is due to the high density of short misfit dislocations, each of which is connected to the layer surface via a pair of threading dislocations (arms). According to Hull et al. [16], even during the initial stage of plastic relaxation, which does not exceed 1%, the TD density in such a sample is at the level of $N_{TD} \sim 10^7$ cm^{-2}, and by the end of plastic relaxation the density increases to 10^8 cm^{-2} (the lower and upper pentagons in Fig. 25, respectively). Positive results in fabricating artificial substrates with a relatively low density of threading dislocations have been attained mainly with heterostructures with a smooth variation of the lattice parameter.

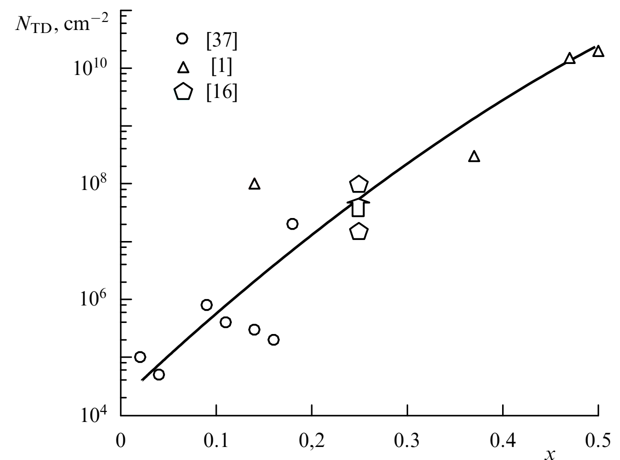

Figure 25. Density of threading dislocations N_{TD} in Ge_xSi_{1-x}/Si(001) layers of constant composition as a function of the germanium concentration x.

5.2.1 Buffer layers with a varying lattice parameter. The method of growing a buffer layer with a varying lattice parameter and a stepwise linearly increasing concentration of the new component of the solid solution has been known for a long time. Over the last 20-odd years this proved to be the most successful way of growing perfect semiconducting layers on substrates with a different lattice parameter. For instance, it is used to fabricate LED arrays on GaAsP/GaAs heterostructures on an industrial scale. Practically all LEDs are fabricated from this material. The main research on these heterostructures was done at the end of the 1960s [119, 120]. The difference in the lattice parameters of the GaAsP layer and the GaAs substrate in the given case did not exceed $\sim 1.5\%$, which was due to the direct-gap part of the GaAsP solid solution necessary for manufacturing effective LEDs.

In the last 10 – 15 years, similar research has been done in order to fabricate GeSi buffer layers on Si. The use of perfect

heterostructures based on GeSi/Si made it possible to substantially improve the properties of devices usually fabricated on silicon substrates (details can be found in the recent reviews by Schäffler [121] and Paul [122]). Another promising feature of such heterostructures is their possible use as artificial substrates for growing GaAs; in the future, this could lead to a combination of devices fabricated on the basis of silicon technology with optoelectronic devices whose main 'building block' is GaAs. Ge_xSi_{1-x}-based buffer layers are the key element of this combination; such buffer layers make it possible to grow strain-relaxed perfect layers of germanium – silicon solid solutions with x up to 1 on their surfaces. Extensive research (e.g., see Refs [6, 113, 123 – 126]) has been devoted to the growing of buffer layers and their structural characteristics.

The advantages of this approach amount to the following: since the composition gradient is chosen to be small (< 0.5% strain per 1 μm), only small elastic strains are present in the buffer layer at each moment. This implies that (a) the layers do not contain large residual stresses if they are grown at temperatures that are not very low; (b) all dislocations injected into a buffer layer are 60° glissile dislocations. The dislocation segments responsible for the compensation of the difference in the lattice parameters of epilayer and substrate are in different planes of the buffer layer. Hence, the interaction between these segments is at its minimum and does not hinder dislocation slip; and (c) the threading dislocations may glide to the edges of the disk, since the effective shear stress in the graded layer is maintained at a certain level.

As a result of intensive studies of the plastic relaxation of strained epilayers in relation to buffer layers with a variable lattice parameter in GeSi/Si heterostructures, a breakthrough in fabricating various semiconductor devices based on Ge_xSi_{1-x}/Si buffer layers with x up to 0.3 (e.g., see the reviews of Schäffler [121] and Paul [122] and the papers cited therein) has become evident.

Unfortunately, when the requirements upon the heterostructures change and become more stringent, the advantages of buffer layers with a varying lattice parameter transform into disadvantages. The smallness of the composition gradient (< 0.5% strain per 1 μm) implies that (a) the buffer layers must be thick (> 1 μm), which makes the growth time longer and increases the consumption of expendables. (König in a paper devoted to forecasting the wider application of heterostructures [129] stated that, economically, a thin (about 100 nm) buffer layer would be ideal); (b) a surface roughness appears that builds-up with thickness and reaches 15 – 20 nm, which constitutes a serious problem in using epilayers in modern technologies; and (c) the dislocation density of $10^6 - 10^7$ cm^{-2} detected in Ge_xSi_{1-x}/Si solid solutions with x close to 1 is fairly high.

Surface roughness is one of the main reasons why the threading dislocation density increases at large values of x. This conclusion was drawn by Fitzgerald et al. [125], who studied the crystalline properties of Ge_xSi_{1-x}/Si buffer layers in a composition interval up to $x = 1$. Valtueña et al. [130] arrive at the same conclusion for InGaAs/GaAs heterostructures. Fitzgerald et al. in a number of recent papers (e.g., see Ref. [113]) related the enhanced TD density in Ge_xSi_{1-x}/Si solid solutions close in composition to pure germanium to the blocking of dispersing MD branches on the steep sections of the rough surface. In this way, the researchers justified one of the main paths of improving the structural perfection of buffer layers with a varying lattice parameter — by strictly maintaining the 2D growth of a buffer layer. To this end they employed the elegant, but hardly practical, mechanochemical polishing of a solid solution of intermediate composition, as a result of which the planarity of the surface was improved [126]. It is in this way that they proved the positive role of the smooth surface of a growing buffer layer: in Ge_xSi_{1-x}/Si solid solutions with x close to 1, the threading dislocation density was lowered by a factor of ten, with the result that high-quality germanium photodiodes integrated on silicon substrates using optimized relaxed graded buffers were fabricated [127]. Samavedam and Fitzgerald [113] discovered that on silicon substrates deviated from the singular face (100) the GeSi buffer layers are smoother and, correspondingly, have better structural properties. This feature was immediately used to fabricate a GaAs/GeSi/Si heterostructure with high electrophysical parameters in the GaAs layer [131].

5.2.2 Mesa substrates (patterned substrates). The closest to the above method of controlling threading dislocations is the one that uses patterned substrates. As early as 1989, Fitzgerald et al. [132] irrevocably proved that reducing the linear dimensions of the mesa region, which shortens the length of MDs fixed at the mesa walls, weakened the interaction and multiplication of the misfit dislocations. This makes h_c larger, a fact proved by experiments. At the same time, for the same reason — because of the weakening of the MD interaction — one should expect a decrease in the threading dislocation density. Despite the fact that a decade has passed since the publication of Ref. [132], no significant progress has been made so far in this path of research [133 – 135], possibly because in the final analysis planar technology should be carefully matched with artificial substrates, which initially have a mesa structure.

5.2.3 Dislocation filters. The filtering properties of separate strained epitaxial layers and strained-layer superlattices (SLSs) in relation to threading dislocations have been known for a long time. These properties are based on the bending of threading dislocations subjected to tangentially directed forces. As a result, a threading dislocation glides to the edge of the epitaxial layer and forms an MD line along the 'strained layer–preceding layer' interface. It is quite logical to use not one strained layer but a system of such layers, i.e., a strained-layer superlattice, to reduce the TD density. In 1976 such an approach was proposed by Matthews et al. [31], and in 1986 Fischer et al. [136] used an InGaAs/GaAs-based superlattice as a dislocation filter in a GaAs/Si heterostructure and found that the TD density was reduced by a factor of ten.

In his review (Ref. [6]), Fitzgerald analyzed this method of reducing the TD density and concluded that the method is ineffective in systems with a high TD density. The explanation is that in such systems (e.g., Ge/Si) the dislocations gliding in large numbers toward the boundary of the epitaxial layer interact, which results in blocking and multiplication, with the result that the reduction of their density does not even exceed a factor of ten. Nevertheless, strained epilayers, SLSs, and recently short-period SLSs as dislocation filters have some use (e.g., see Refs [137, 138]).

The use of single layers also yields rather good results in reducing the TD density. For instance, Osten and Bugiel [139] describe growing the $Ge_{0.3}Si_{0.7}$ solid solution on Si(001) with the use of buffer layers with 10, 15, 20, and 25% Ge. The TD density in the upper layer was 10^7 cm^{-2}. After a ternary

GeSiC solid solution was 'inserted' into each buffer layer consisting of the GeSi solid solution (with the ternary solid solution matched to it), the TD density was found to reduce to a value smaller than 10^5 cm^{-2}. The researchers assume that, in the intermediate annealing of each such heterostructure, the threading dislocations, which glide toward the periphery of the layers, bend because of their slower motion through the GeSiC layer and settle themselves mainly along the interface between the GeSi and GeSiC solid solutions, which are matched in the lattice parameters.

5.3 Silicon – germanium nanostructures with quantum dots

Strained-layer superlattices Si/GeSi and nanostructures with quantum dots constitute an important example of heterostructures containing layers that are in an elastically strained defect-free state. Despite the large difference in the lattice parameters, such heterostructures attract the attention of applied scientists because of the great progress achieved in fabricating new devices that employ quantum effects. The fabrication of light-emitting and light-sensitive silicon – germanium devices is an example of the successful competition of silicon SLSs and conventional optoelectronic materials, such as III – V compounds. The interest in Ge and Si nanoclusters is caused by a number of circumstances: (a) a technology has been developed for fabricating spatially homogeneous arrays of germanium nanoclusters, (b) it has been made possible to reduce the nanocluster size to values that ensure the manifestation of size-quantization and electron – electron interaction effects up to room temperature, and (c) the new methods are compatible with the existing silicon technology to fabricate discrete circuits and devices.

Such developments, until now considered quite exotic, may lead to a revolution in silicon integrated-circuit technology.

Until 1992, the main method of fabricating structures in which the researchers were able to achieve size quantization of charge carriers was photolithography, with its inherent limitations on the minimum size. The discovery of ordering effects in arrays of nanometer islands in Ge/Si and InAs/GaAs heterostructures made it possible to produce defect-free quantum dots of minimum dimensions (10 – 100 nm) with a density of $10^{10} - 10^{11}$ cm^{-2} and led to a clearer exposure of the atomlike nature of the electronic and optical spectra of these objects. After the first publications, there was an upsurge of research into the mechanisms of formation of strained islands and of the ordering of such islands, since this opens the possibility of fabricating arrays of defect-free (without misfit dislocations) 3D objects of nanometer dimensions, objects that hold much promise for nanoelectronics applications.

The development and the modern state of the ideas about the ordering of ensembles of quantum dots in heteroepitaxial processes have been thoroughly covered in the reviews by Pchelyakov et al. [140]. The researchers discussed the driving forces for, and the main mechanisms of, the evolution and ordering of nanometer-sized objects in heterosystems with a large mismatch of the lattice parameters in the course of molecular-beam epitaxy and thermal treatment. They analyzed the experimental data on cluster formation and self-organization of Ge/Si nanostructures on silicon surfaces and discussed possible ways of ordering the structures and reducing the size and increasing the density of silicon quantum dots. They also presented the results of studies of the electronic and optical properties of heterostructures and multilayer composites with germanium quantum dots.

6. Conclusion

In this review, we have generalized the achievements of researchers over the last 10 – 15 years in understanding the relaxation of strained epilayers, both plastic relaxation and elastic relaxation, in relation to GeSi solid solutions on silicon. It is with this material grown by molecular-beam epitaxy that the main features of nucleation and propagation of misfit dislocations, which lead to plastic relaxation of strained semiconductor layers and multilayer heterostructures, have been studied. The GeSi/Si system also appears to be the most important in studies of the formation of ensembles of elastically relaxed 3D clusters of nanometer sizes (e.g., see the reviews by Pchelyakov et al. [140]).

The achievements in understanding the laws governing the injection, propagation, and annihilation of dislocations in initially strained GeSi/Si layers made it possible to fabricate transistor structures with new electronic properties and totally strain-relaxed compositions such as artificial substrates, on which growing GaAs became possible, and in this way to merge silicon technology with the main material of optoelectronics. However, despite the important advances in the phenomenological description of the relaxation of strained layers via MD injection, we are still far away from a complete understanding of this process. For the time being, the fact that plastic relaxation of pseudomorphic layers is a complex process incorporating many factors and having many stages complicates the building of a consistent mathematical model. The process of MD nucleation on the atomic level also requires serious investigation.

In the last five years, the interest of researchers in the formation of island epilayers has grown dramatically. This phenomenon has triggered a lot of interest in the scientific and engineering community due to the simple fact that it opens the possibility of fabricating defect-free 3D centers of high density ($> 10^{10}$ cm^{-2}) with dimensions ensuring the emergence of size-quantization and electron – electron interaction effects up to room temperature. The elastic relaxation of strains in epitaxial layers and 3D germanium islands on silicon is the key factor ensuring the morphological transition of a planar layer into an island layer. The inhomogeneity of strain relaxation and the dependence of strain on the shape and size of the islands affect the subsequent stages in the evolution of 3D centers, including their density and spatial distribution. This phenomenon has been actively discussed in the literature and is briefly studied in the present review as one of the real paths of defect-free strain relaxation in epilayers.

In the last decade, new approaches to layer relaxation have been developed. They are based on the redistribution of strains between the growing layer and the thin (or soft) membranous substrate, and do not require MD injection. The fact that dislocation-free relaxation of layers can be achieved through the use of various membranous substrates has been demonstrated many times. However, the problems of elastic relaxation of perfect epilayers grown on large semiconductor substrates used in epitaxial technology have yet to be solved.

Acknowledgments. This work was supported in part by the Russian Foundation for Basic Research (project Nos. 00-02-17690 and 00-02-17638), the Leading Scientific Schools of Russia Program (project No. 00-15-96806), the Perspective Technologies and Devices for Micro- and Nanoelectronics Program, and INTAS (grant Nos. 97-10628 and 99-00125).

References

1. Kvam E P, Maher D M, Humphreys C J *J. Mater. Res.* **5** 1900 (1990)
2. Frank F C, Van der Merwe J H *Proc. Roy. Soc. London Ser. A* **198** 205 (1949)
3. Matthews J W *J. Vac. Sci. Technol.* **12** 126 (1975)
4. Gillard V T, Nix W D, Freund L B *J. Appl. Phys.* **76** 7280 (1994)
5. Matthews J W, Blakeslee A E *J. Cryst. Growth* **27** 118 (1974)
6. Fitzgerald E A *Mater. Sci. Rep.* **7** 87 (1991)
7. Fisher A *Appl. Phys. Lett.* **64** 1218 (1994)
8. Gutakovskiĭ A K, Pchelyakov O P, Stenin S I *Kristallografiya*. **25** 806 (1980) [*Sov. Phys. Crystallogr.* **25** 461 (1980)]
9. Green M L et al. *J. Appl. Phys.* **69** 745 (1991)
10. Houghton D C et al. *Appl. Phys. Lett.* **56** 460 (1990)
11. Houghton D C et al. *J. Appl. Phys.* **67** 1850 (1990)
12. People R, Bean J C *Appl. Phys. Lett.* **47** 322 (1985)
13. Bolkhovityanov Yu B et al. *Thin Solid Films* (2001) (in press)
14. Bai G et al. *J. Appl. Phys.* **75** 4475 (1994)
15. Hirth J P, Lothe J *Theory of Dislocations* 2nd ed. (New York: Wiley, 1982)
16. Hull R, Bean J C, Buescher C *J. Appl. Phys.* **66** S837 (1989)
17. Hull R et al. *Appl. Phys. Lett.* **65** 327 (1994)
18. Stach E A et al. *J. Appl. Phys.* **83** 1931 (1998)
19. Hull R et al. *Phys. Stat. Solidi A* **171** 133 (1999)
20. Houghton D C *J. Appl. Phys.* **70** 2136 (1991)
21. Perovic D D, Houghton D C *Inst. Phys. Conf. Ser.* **146** 117 (1995)
22. Alexander H, Haasen P *Solid State Phys.* **22** 27 (1968)
23. Farber B Ya, Iunin Yu L, Nikitenko V I *Phys. Stat. Solidi A* **97** 469 (1986)
24. Iunin Yu L et al. *Zh. Eksp. Teor. Fiz.* **100** 1951 (1991) [*Sov. Phys. JETP* **73** 1079 (1991)]
25. Iunin Yu L, Nikitenko V I *Phys. Stat. Solidi A* **171** 17 (1999)
26. Yonenaga I *Phys. Stat. Solidi A* **171** 41 (1999)
27. Perovic D D et al. *Thin Solid Films* **183** 141 (1989)
28. Wickenhauser S et al. *Appl. Phys. Lett.* **70** 324 (1997)
29. Stach E A et al. *Microsc. Microanal.* **4** 294 (1998)
30. Jain S C et al. *J. Appl. Phys.* **87** 965 (2000)
31. Matthews J W, Blakeslee A E, Mader S *Thin Solid Films* **33** 253 (1976)
32. Kamat S V, Hirth J P *J. Appl. Phys.* **67** 6844 (1990)
33. Eaglesham D J et al. *Philos. Mag. A* **59** 1059 (1989)
34. Hull R, Bean J C *J. Vac. Sci. Technol. A* **7** 2580 (1989)
35. Mooney P M et al. *J. Appl. Phys.* **75** 3968 (1994)
36. Beanland R *J. Appl. Phys.* **77** 6217 (1995)
37. Vdovin V I *Phys. Stat. Solidi A* **171** 239 (1999)
38. Jain S C, Willander M, Maes H *Semicond. Sci. Technol.* **11** 641 (1996)
39. Tersoff J, LeGoues F K *Phys. Rev. Lett.* **72** 3570 (1994)
40. Shchukin V A, Bimberg D *Appl. Phys. A* **67** 687 (1998)
41. Ozkan C S, Nix W D, Gao H *Appl. Phys. Lett.* **70** 2247 (1997)
42. Cullis A G, Pidduck A J, Emeny M T *J. Cryst. Growth* **158** 15 (1996)
43. Hu S M *J. Appl. Phys.* **69** 7901 (1991)
44. Matthews J W, Mader S, Light T B *J. Appl. Phys.* **41** 3800 (1970)
45. Dodson B W, Tsao J Y *Appl. Phys. Lett.* **51** 1325 (1987); **52** 852 (1988)
46. Fox B A, Jesser W A *J. Appl. Phys.* **68** 2801 (1990)
47. Jesser W A, Fox B A *J. Electron. Mater.* **19** 1289 (1990)
48. Hull R, Bean J C *Appl. Phys. Lett.* **54** 925 (1989)
49. Gillard V T, Nix W D, Freund L B *J. Appl. Phys.* **76** 7280 (1994)
50. Freund L B *J. Appl. Phys.* **68** 2073 (1990)
51. Fitzgerald E A et al. *Phys. Stat. Solidi A* **171** 227 (1999)
52. Fisher A et al. *Phys. Rev. B* **54** 8761 (1996)
53. Hagen W, Strunk H *Appl. Phys.* **17** 85 (1978)
54. Rajan K, Denhoff M *J. Appl. Phys.* **62** 1710 (1987)
55. Vdovin V I (private communication)
56. Beanland R *J. Appl. Phys.* **72** 4031 (1992)
57. LeGoues F K, Meyerson B S, Morar J F *Phys. Rev. Lett.* **66** 2903 (1991)
58. LeGoues F K *Phys. Rev. Lett.* **72** 876 (1994)
59. Capano M A *Phys. Rev. B* **45** 11768 (1992)
60. Tuppen C G, Gibbings C J, Hockly M *J. Cryst. Growth* **94** 392 (1989)
61. Houghton D C et al. *J. Appl. Phys.* **67** 1850 (1990)
62. Liu J L et al. *Appl. Phys. Lett.* **75** 1586 (1999)
63. Vdovin V I *J. Cryst. Growth* **172** 58 (1997)
64. Gosling T J *J. Appl. Phys.* **74** 5415 (1993)
65. Dentel D et al. *J. Cryst. Growth* **191** 697 (1998)
66. Gosling T J et al. *J. Appl. Phys.* **73** 8267 (1993)
67. Houghton D C, Davies M, Dion M *Appl. Phys. Lett.* **64** 505 (1994)
68. Tkhorik Yu A, Khazan L S *Plasticheskaya Deformatsiya i Dislokatsii Nesootvetstviya v Geteroepitaksial'nykh Sistemakh* (Plastic Strain and Misfit Dislocations in Heteroepitaxial Systems) (Kiev: Naukova Dumka, 1983) p. 135
69. Freund L B, Nix W D *Appl. Phys. Lett.* **69** 173 (1996)
70. Zhang T Y, Su Y J *Appl. Phys. Lett.* **74** 1689 (1999)
71. Lo Y H *Appl. Phys. Lett.* **59** 2311 (1991)
72. Powell A R, LeGoues F K, Iyer S S *Appl. Phys. Lett.* **64** 324 (1994)
73. Brunner K et al. *Thin Solid Films* **321** 245 (1998)
74. Antypas G A, Edgecumbe J *Appl. Phys. Lett.* **26** 371 (1975)
75. Lau W S et al. *Jpn. J. Appl. Phys.* **36** 3770 (1997)
76. Carter-Coman C et al. *Appl. Phys. Lett.* **70** 1754 (1997)
77. Ejeckam F E et al. *Appl. Phys. Lett.* **71** 776 (1997)
78. Kästner G, Gösele U, Tan T Y *Appl. Phys. A* **66** 13 (1988)
79. Jesser W A, van der Merwe J H, Stoop P M *J. Appl. Phys.* **85** 2129 (1999)
80. Bellet D, in *Properties of Porous Silicon* (Ed. L Carnham) (London: INSPEC, 1997) p. 127
81. Romanov S I et al. *Appl. Phys. Lett.* **75** 4118 (1999)
82. Asaro R J, Tiller W A *Metall. Trans.* **3** 1789 (1972)
83. Grinfel'd M A *Dokl. Akad. Nauk SSSR* **290** 1358 (1986) [*Sov. Phys. Dokl.* **31** 831 (1986)]
84. Berger P R et al. *Appl. Phys. Lett.* **53** 684 (1988)
85. Srolovitz D J *Acta Metall.* **37** 621 (1989)
86. Eaglesham D J, Cerullo M *Phys. Rev. Lett.* **64** 1943 (1990)
87. Guha S, Madhukar A, Rajkumar K C *Appl. Phys. Lett.* **57** 2110 (1990)
88. Mo Y W et al. *Phys. Rev. Lett.* **65** 1020 (1990)
89. Snyder C W et al. *Phys. Rev. Lett.* **66** 3032 (1991)
90. Cullis A G et al. *J. Cryst. Growth* **123** 333 (1992)
91. Ratsch C, Zangwill A *Surface Sci.* **293** 123 (1993)
92. Spencer B J, Voorhees P W, Davis S H *J. Appl. Phys.* **73** 4955 (1993)
93. Freund L B, Jonsdottir F *J. Mech. Phys. Solids* **41** 1245 (1993)
94. Johnson H T, Freund L B *J. Appl. Phys.* **81** 6081 (1997)
95. Obayashi Y, Shintani K *J. Appl. Phys.* **84** 3142 (1998)
96. Müller P, Kern R *J. Cryst. Growth* **193** 257 (1998)
97. Kern R, Müller P *Surface Sci.* **392** 103 (1997)
98. Moll N, Scheffler M, Pehlke E *Phys. Rev. B* **58** 4566 (1998); Pehlke E et al. *Appl. Phys. A* **65** 525 (1997)
99. Kamins T I et al. *J. Appl. Phys.* **85** 1159 (1999)
100. Floro J A et al. *Phys. Rev. B* **59** 1990 (1999)
101. Ozkan C S, Nix W D, Gao H *Appl. Phys. Lett.* **70** 2247 (1997)
102. Dentel D et al. *J. Cryst. Growth* **191** 697 (1998)
103. Lafontaine H et al. *J. Vac. Sci. Tech. B* **16** 599 (1998)
104. Jesson D E et al. *Phys. Rev. Lett.* **71** 1744 (1993)
105. Dorsch W et al. *Appl. Phys. Lett.* **72** 179 (1998)
106. Cullis A G, Pidduck A J, Emeny M T *Phys. Rev. Lett.* **75** 2368 (1995)
107. Cullis A G, Pidduck A J, Emeny M T *J. Cryst. Growth* **158** 15 (1996)
108. Peiro F et al. *Appl. Phys. Lett.* **74** 3818 (1999)
109. Gao H et al. *Philos. Mag. A* **79** 349 (1999)
110. Gallas B et al. *J. Cryst. Growth* **201/202** 547 (1999)
111. Olsen G H *J. Cryst. Growth* **31** 223 (1975)
112. Lutz M A et al. *Appl. Phys. Lett.* **66** 724 (1995)
113. Samavedam S B, Fitzgerald E A *J. Appl. Phys.* **81** 3 108 (1997)
114. Dargys A, Kundrotas J *Handbook on Physical Properties of Ge, Si, GaAs and InP* (Vilnius: Science and Encyclopedia Publ., 1994)
115. Liu L, Lee C S, Marshak A H *Solid State Electron.* **37** 421 (1994)
116. Whall T E, Parker E H C *Thin Solid Films* **367** 250 (2000)
117. König V, Glück M, Höck G *J. Vac. Sci. Technol. B* **16** 2609 (1998)
118. Ahlgren D C, Jagannathan B *Solid State Technol.* **43** 53 (2000)
119. Abrahams M S et al. *J. Mater. Sci.* **4** 223 (1969)
120. Burd J W *Trans. Metall. Soc. AIME* **245** 571 (1969)
121. Schäffler F *Semicond. Sci. Technol.* **12** 1515 (1997); *Thin Solid Films* **321** 1 (1998)
122. Paul D J *Thin Solid Films* **321** 172 (1998)
123. Fitzgerald E A et al. *Appl. Phys. Lett.* **59** 811 (1991)
124. Schäffler F et al. *Semicond. Sci. Technol.* **7** 260 (1992)

125. Fitzgerald E A et al. *J. Vac. Sci. Technol. A* **15** 1048 (1997)
126. Currie M T et al. *Appl. Phys. Lett.* **72** 1718 (1998)
127. Samavedam S B et al. *Appl. Phys. Lett.* **73** 2125 (1998)
128. Iwano H et al. *Thin Solid Films* **317** 17 (1998)
129. König U *Phys. Scripta* **68** 90 (1996)
130. Valtueńa J F et al. *J. Cryst. Growth* **182** 281 (1997)
131. Sieg R M et al. *Appl. Phys. Lett.* **73** 3111 (1998)
132. Fitzgerald E A et al. *J. Appl. Phys.* **65** 2220 (1989)
133. Noble D B et al. *Appl. Phys. Lett.* **56** 51 (1990)
134. Hammond R et al. *Appl. Phys. Lett.* **7**1 2517 (1997)
135. Rupp T et al. *Thin Solid Films* **294** 27 (1997)
136. Fischer R et al. *J. Appl. Phys.* **60** 1640 (1986)
137. Samonji K et al. *Appl. Phys. Lett.* **69** 100 (1996)
138. Obata T et al. *J. Appl. Phys.* **81** 199 (1997)
139. Osten H J, Bugiel E *Appl. Phys. Lett.* **70** 2813 (1997)
140. Pchelyakov O P et al. *Thin Solid Films* **367** 75 (2000); Pchelyakov O P *Fiz. Tekh. Poluprovodn.* **34** 1281 (2000) [*Semiconductors* **34** 1229 (2000)]